Biomaterials Science

ROYAL SOCIETY OF CHEMISTRY

REVIEW

View Article Online
View Journal | View Issue

Cite this: *Biomater. Sci.*, 2023, **11**, 356

Recent advances in responsive antibacterial materials: design and application scenarios

Bo Zhang, Derong Lu and Hongwei Duan *

Bacterial infection is one of the leading causes of death globally, although modern medicine has made considerable strides in the past century. As traditional antibiotics are suffering from the emergence of drug resistance, new antibacterial strategies are of great interest. Responsive materials are appealing alternatives that have shown great potential in combating resistant bacteria and avoiding the side effects of traditional antibiotics. In this review, the responsive antibacterial materials are introduced in terms of stimulus signals including intrinsic (pH, enzyme, ROS, *etc.*) and extrinsic (light, temperature, magnetic fields, *etc.*) stimuli. Their biomedical applications in therapeutics and medical devices are then discussed. Finally, the author's perspective of the challenge and the future of such a system is provided.

Received 28th September 2022,
Accepted 14th November 2022

DOI: 10.1039/d2bm01573k

rsc.li/biomaterials-science

1. Introduction

Although the pandemic of the coronavirus disease 19 (Covid-19) was the world's most concerning disease during the past two years, the infection of the other kind of microorganism, bacteria, has always been a leading cause of death around the world. The discovery of penicillin in the early 20th century launched the new era of antibiotics that vastly extended the human lifespan, however, the misuse of antibiotics accelerated the evolution of bacteria, thereby the development of antimicrobial resistance (AMR).[1,2] As one of the primary public health threats faced by modern society, AMR was estimated to cause global mortality of 4.95 million during the year 2019 alone and is projected to kill as many as 10 million people each year by 2050.[3,4] Other than the AMR, some of the antibiotics are also challenged by the adverse side effect resulting from hypersensitivity reaction, direct cytotoxicity, and the damage to the beneficial gut microbiome.[5,6] As the discovery of new antibiotics can hardly keep up with the rapidly emerging AMR and the adverse reactions becoming more concerning, numerous research efforts have been focused on alternative strategies such as the exploitation of antimicrobial pep-

School of Chemistry, Chemical Engineering and Biotechnology, Nanyang Technological University, 70 Nanyang Drive, Singapore 637457, Singapore. E-mail: hduan@ntu.edu.sg

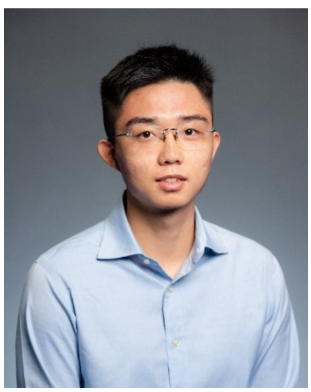

Bo Zhang

Bo Zhang obtained his undergraduate degree in pharmaceutical sciences at Peking University, China. Now he is a Ph.D. candidate in chemical and biomedical engineering under Prof. Hongwei Duan's supervision at Nanyang Technological University, Singapore. His current research focuses on the development of enzyme-responsive system to improve the existing biocidal agents against drug-resistant bacterial infection.

Derong Lu

Derong Lu received his B.S. and M.S. in polymer chemistry & physics at National Huaqiao University, China. He obtained Ph.D. degree in polymer chemistry & physics at University of Queensland in 2016, under supervision of Professor Michael J. Monteiro. Since 2016, he joined in Prof. Hongwei Duan's group and working as a postdoctoral research fellow at Nanyang Technological University, Singapore. His research focuses on the synthesis of well-defined functional polymers and nanocrystals, the self-assembly of polymer coated plasmonic nanocrystals, and the synthesis of biodegradable antibacterial polymers.

tides (AMPs),[7,8] bacteriolytic enzymes,[9,10] and the stimuli-responsive antibacterial materials.

Responsive biomaterials that are sensitive to physiological, pathological, or external stimuli can be activated by these signals and are considered promising therapeutic platforms for the next-generation precision medication.[11] Manifold strategies have been employed for this kind of material. A common strategy is to deliver therapeutics in spatial- and temporal-controlled manners to precisely target the sites of interest, thus improving the pharmacokinetic profiles and reducing the off-target adverse effects.[12] The other one is to transduce triggering signals to generate therapeutic effects. For example, optical signals can be absorbed by photothermal agents to produce localized heat in photothermal therapies.[13,14] Likewise, modulation of bio-interfaces can be achieved by stimuli-responsive coatings, represented by thermally triggered cell-sheet engineering and biocidal coatings.[15–17] Stimuli-responsive materials have shown great potential for the treatment of major human diseases, such as cancer,[18,19] cardiovascular diseases,[20,21] and bacterial infections.[22]

The antibacterial application of responsive materials has received growing attention, as evidenced by an increasing tendency in the number of publications during the past two decades (the histogram in Fig. 1). We will focus on the research in the past five years, and their design and biomedical application scenarios will be summarized. The classification of such materials varies based on different grounds. In terms of dimensions and physical forms, nanoparticles,[23] hydrogels,[24] and surfaces[25] have all been widely explored. This review focuses on stimuli-responsive properties. As such, the materials are classified by the stimulus signals which they respond to, namely, the intrinsic stimuli that exist at the infectious site (*i.e.*, pH and enzyme) and the extrinsic stimuli that are applied externally (light, magnetic fields, *etc.*). Their biomedical applications and their treatment outcomes are then discussed (Fig. 1).

Hongwei Duan

Hongwei Duan is a professor at the School of Chemistry, Chemical Engineering and Biotechnology at Nanyang Technological University. He received his B.S. in applied chemistry and M.S. in polymer chemistry and physics from Fudan University. After completing his Ph.D. at the Max Planck Institute of Colloids and Interfaces, he had his postdoctoral training in the joint Department of Biomedical Engineering at Emory University and Georgia Institute of Technology. His current research focuses on understanding surface/interface properties of micro- and nanostructures to achieve tailored optical, electronic, magnetic, catalytic, and structural properties for biomedical and environmental applications.

2. Intrinsic stimuli

A particular microenvironment would be formed when bacteria colonize and propagate in the human body, arising from the pathogen-secreted metabolites or infection-induced inflammation. Combined with some unique physiological conditions in specific organs, these abnormities can be employed as endogenous triggers to activate the antibacterial activities of stimuli-responsive materials. This section presents the introductions of specific stimuli and corresponding responsiveness, and primarily focuses on the design of the materials rather than the therapeutic efficacy.

2.1 pH

Over millions of years of evolution, certain bacteria have acquired the ability to thrive in highly acidic environments. For example, *Helicobacter pylori* can inhabit extracellularly in the human stomach with a median pH of 1.4,[26] and *Mycobacterium tuberculosis*, *Francisella tularensis*, and *Listeria monocytogenes* are known to thrive intracellularly in the phagolysosomes with a pH of 4.5–5.[27] In addition, bacteria can also survive in other naturally acidic organs like vaginas (pH ≈ 4),[28] skins (pH ≈ 5),[29] and bladders (pH ≈ 6).[30] Apart from those natural acidic environments, an acidic microenvironment can also be generated due to the presence of bacteria's anaerobically metabolic products, such as acetic acids secreted by *Escherichia coli* and lactic acids secreted by *Staphylococcus aureus*.[31–33] Those characteristics provide feasibility to design pH-responsive systems for antimicrobial purposes. Classified by functions, the pH-responsiveness can boost antimicrobial properties mainly by (i) pH-induced release, (ii) pH-trigged chemical conversion, and (iii) pH-induced aggregation.

2.1.1 pH-Induced release. Bactericidal agents can be loaded in a pH-responsive carrier, which offers an opportunity to realize targeted delivery and controlled release of drug, as well as deprotection for encapsulated cargo. Conjugating antibacterial drugs to the polymeric carriers through a pH-liable chemical bonds is a common strategy that afford a relatively high loading efficiency. Such bonds are readily cleaved in an acidic microenvironment, followed by the release of cargo. Imine bond that containing a carbon nitrogen double bond (–CH=N–) can be easily hydrolyzed at acidic environment[34] Yang *et al.* reported a one-pot fabrication of a semi-2D coating containing two natural antibacterial molecules, protocatechualdehyde (PA) and aminoglycosides (AGs). In this design, phenyl hydroxyl group on the PA backbone enable a firm adhesion between PA and subtract, while its aldehyde functionality afford *in situ* formation of imine bond between PA and amine-group containing AGs, giving rise to a 2D coating layer as shown in Fig. 2A.[35] In an acidic condition (*e.g.*, pH = 5), the AGs exhibited a much faster release rate than that of in physiological conditions (pH = 7.4), as a result of the degra-

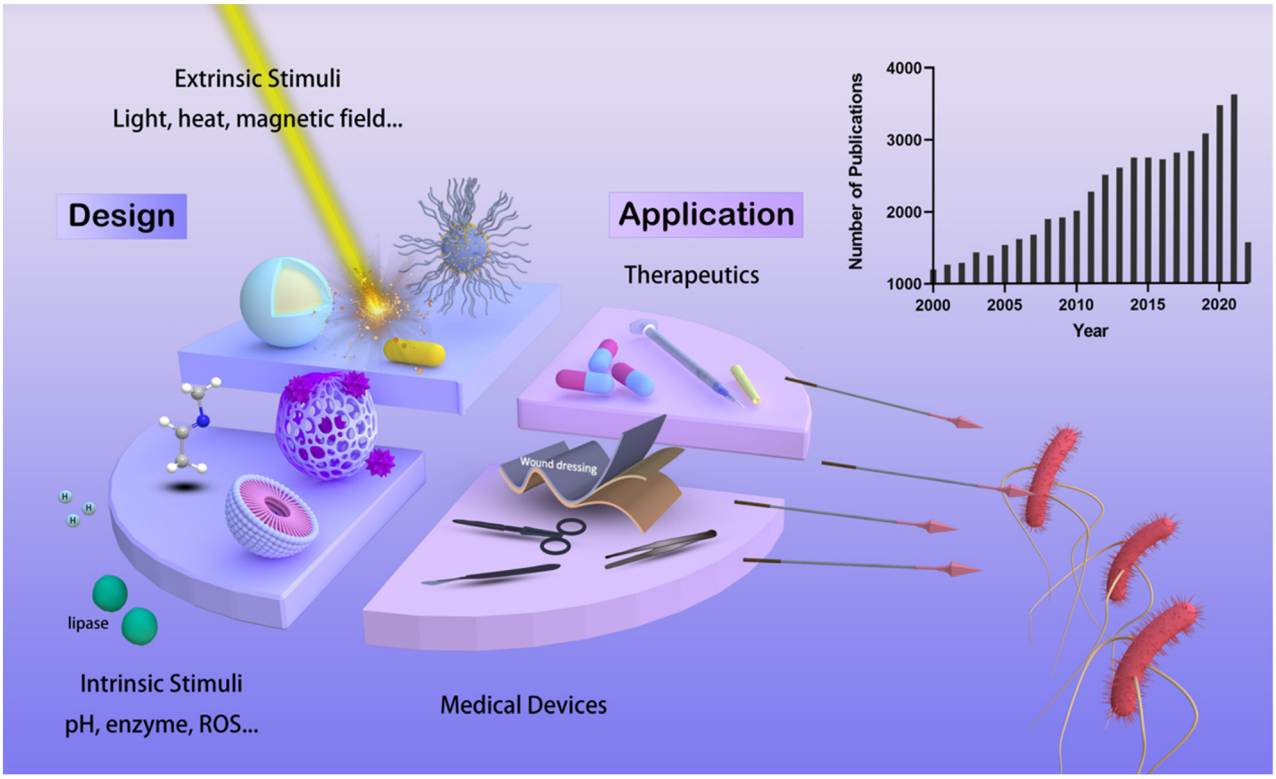

Fig. 1 Schematic illustration of the overview on the responsive antibacterial materials. The histogram was generated by searching for the keywords "responsive antibacterial" on the PubMed database. The stimuli-responsive antibacterial materials can be classified according to the signals they respond to: intrinsic stimuli-sensitive materials (*i.e.,* micelles and porous drug-loading particles) (lower left quarter of the pie figure) and extrinsic stimuli materials (*i.e.,* core–shell particles and plasmonic gold nanorods) (upper left quarter of the pie figure). These materials can be applied as directed therapeutics against bacterial infection (upper right of the pie figure) and used in medical devices including wound healing and implants materials (lower right of the pie figure).

dation of imine bonds. Similarly, Hu *et al.* reported a hydrogel prepared by the crosslinking oxidized dextran with amine-abundant tobramycin and G1-orni (prodrug of ornidazole) *via* the acid-labile imine linkages.[36] The release of tobramycin and G1-orni from the hydrogel in a pH 5.0 buffer mimicking the bacterial suspension were faster in speed and more in quantity than in a pH 7.4 buffer. Besides imine bonds, other pH-liable linkages including hemiaminal ether bonds,[37] boronate ester bonds,[38] β-carboxylic acid amides,[39] and acetal bonds[40] were also exploited for responsive release of cargos ranging from small molecule antibiotics to macromolecular antimicrobial peptides (AMPs).

Another popular strategy for antibacterial cargo release is through pH-responsive decay of the encapsulating materials, including pH-induced swelling and collapsing. pH-Induced swelling is mainly caused by electric repulsion between protonated groups in acidic environment or deprotonated groups in alkaline environments. Chitosan (CS), a linear polysaccharide that is rich in amino groups, has been widely studied to endow encapsulating materials with swelling properties. Hao *et al.* developed an antibacterial multilayer film consisting of capsaicin (CAP)@CS nanocapsules where antibiotic CAP was encapsulated within the CS network.[41] Under acidic conditions, the CS network was swelled and thus released the CAP as a result of the electrostatic repulsion of protonated amino groups. While under basic conditions, the polymer network shrank due to deprotonation of amino groups associated with less drug releasing. Similarly, Liang *et al.* encapsulated amoxicillin into an injectable hydrogel formed by chitosan-grafted-dihydrocaffeic acid and oxidized pullulan.[42] The amino groups in chitosan were protonated and exhibit positive charge in acidic PBS (pH 5.5), thus repulsed to each other. Moreover, the Schiff base bonds as crosslinkers were also weakened in acidic solution, causing the hydrogel to swell and lead to controlled release of amoxicillin. Interestingly, CS-containing materials can also respond to increased pH for drug release. For example, in a CS-containing coating material, when pH increases as in the wound site, the number of protonated amino groups ($-NH_3^+$) in CS decreases, leading to the dissociation of ionic bonds in the complex network., This caused an increased swelling of the complex coating and the drug release.[43]

Different from swelling, the coating materials for pH-induced degradation happen primarily in systems containing inorganic nanoparticles. For instance, Ag nanoparticles cluster (AgNC) was synthesized using polymers containing *ortho* ester

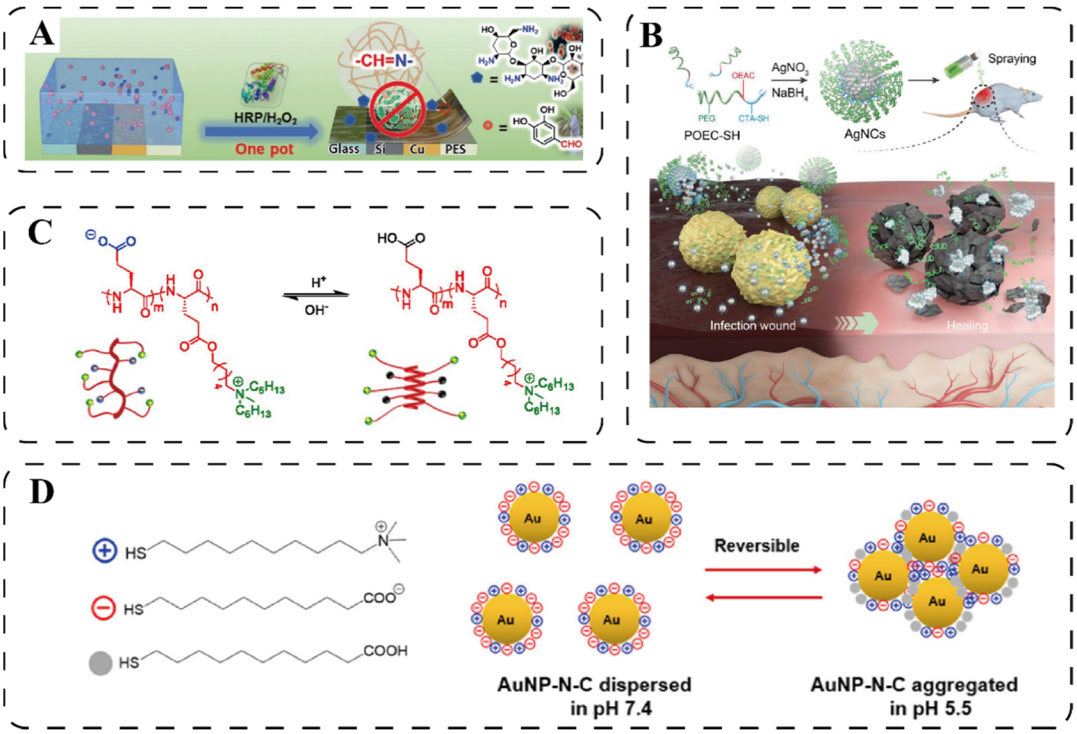

Fig. 2 (A) Schematic illustration of the pH-sensitive antibacterial coating for controlled release of antibiotics. Reprinted with permission from ref. 35. Copyright 2021, Wiley-VCH. (B) The synthesis and the pH-induced collapsing of the AgNC. Reprinted with permission from ref. 44. Copyright 2020, Wiley-VCH. (C) The pH-activated conformation transition of HCT-AMPs. Reprinted with permission from ref. 48. (D) The surface charge of the AuNP-N-C changed to positive under the acidic infectious microenvironment due to the protonation of $-NH_2$ and $-COO^-$. Reproduced with permission from ref. 23. Copyright 2017, American Chemical Society.

segments, which could be hydrolyzed by acid, leading to the release of Ag nanoparticles as shown in Fig. 2B.[44] In another work, bactericidal berberine-loaded ZnO nanosphere was coated by a pH-sensitive zeolitic imidazolate framework (ZIF). Under a weak acid environment, the ZIF shell gradually degrade to expose ZnO nanosphere and lease berberine.[45] In addition, calcium carbonate ($CaCO_3$) coating could be dissolved upon reacting with acid, and consequently exposing the cargo inside.[46,47] Notably, if the dissolution of $CaCO_3$ occurs in a phosphate-containing environment, a more stable $Ca_3(PO_4)_2$ coating would be form in the presence of free Ca^{2+}. As a result, further dissolution of inner $CaCO_3$ would be inhibited due to the protecting effect of as-formed $Ca_3(PO_4)_2$ surface layer.[46] In this case, therefore, the release kinetic of drug can be affected when using phosphate-rich buffer, which should be taken into account in the experiment design.

However, a common problem faced by many of abovementioned delivery systems is the nonspecific drug release at physiological pH, stemming from poor stability of corresponding linkages at the neutral pH. In the extreme case, up to 70% of drug is released before the delivering carriers arrives targeting infection sites.[40] The off-target toxicity could occur in a systemic delivery model. Thus, choosing the pH-sensitive linkage that is highly stable in the physiological condition (pH = 7.4) remains challenging for the development of pH-responsive antibacterial systems.

2.1.2 pH-Induced conversion. Unlike loading an antibacterial agent into a carrier, the concept of pH-induced conversion is that originally non-toxic molecules can be converted into a bactericidal form in the presence of H^+, which can avoid the off-target release of drugs mentioned in the previous sector. One approach to this end is pH-induced protonation. As shown in Fig. 2C, Xiong *et al.* reported pH-responsive AMPs with a helix–coil conformation transition (HCT-AMPs).[48] The HCT-AMPs were in random coiled conformation at physiological pH resulting from the electrostatic interaction between the anionic carboxylate and cationic amine groups. In contrast, under acidic conditions, it was converted to a helical conformation due to the protonation of carboxylate groups and depletion of side-chain electrostatic interactions. Such helical conformation led to potent antibacterial efficacy against *H. pylori* in the stomach. The H^+-triggered protonation of the tertiary amine in polymers to quaternary ammonium is also a popular strategy,[49,50] as the transformed cationic polymers are known to disrupt negatively-charged bacterial cell membranes by electrostatic interactions.[51] In addition to protonation-induced conversion, H^+ can also act as a reactant to generate bactericidal agents. For example, Zu *et al.* incorporated copper peroxide (CuO_2) nanoparticles into hydrogels to achieve a synergistic enhanced Fenton reaction.[52] The H^+ in the infection site could react with CuO_2 and generate Cu^{2+} and H_2O_2. Subsequently, Cu^{2+} was reduced by glutathione (GSH) to Cu^+,

which could catalyze the self-supplied H_2O_2 to form highly toxic hydroxyl radical ($^{\bullet}OH$).

2.1.3 pH-Induced aggregation. The membrane of most bacterial cells are negatively charged, attributing to the presence of phosphate group-rich teichoic acids in Gram-positive bacteria and lipopolysaccharides in Gram-negative ones.[53] Positively charged materials can electrostatically bind to the negatively charged bacterial cell surface, thereby causing the accumulation of the materials. By taking advantage of this enrichment, other antibacterial strategies such as photothermal therapy (PTT),[54] photodynamic therapy (PDT),[55] or localized drug release[55] can be integrated to boost their efficacy through enhanced local concentration of materials. The positive charge of the antibacterial materials can be introduced by their surface charge reversal in response to pH changes. For example, Hu *et al.* developed a surface-adaptive zwitterionic gold nanoparticle (AuNP-N-C) fabricated from the self-assembly of strong electrolytic (10-mercaptodecyl)trimethylammonium bromide (HS-C_{10}-N_4) and weak electrolytic 11-mercaptoundecanoic acid (HS-C_{10}-COOH), as illustrated in Fig. 2D.[23] At neutral pH, the AuNP-N-C exhibited a negatively charged surface, while in Methicillin-resistant *Staphylococcus aureus* (MRSA) biofilm with pH 5.5, the surface of the AuNPs reversibly changed into positive due to the protonation of both $-NH_2$ to form $-NH_3^+$ and $-COO^-$ to –COOH. Consequently, the charge-reversed AuNPs could effectively adhere to the bacterial surface and showed excellent antibacterial efficacy under near-infrared (NIR) light irradiation.

2.2 Enzyme

Nutrients like saccharides, peptides, and nucleic acids often exist as oligomers or macromolecules in nature. Most bacteria are capable of secreting enzymes into surroundings to digest those macromolecules into smaller fragments so that the partially digested nutrients can be internalized into the bacterial cells.[56] In addition to nutrition, bacteria also secret enzymes to survive against the host's defence mechanism and promote invasion. For example, the over-expressed lipase secreted by *S. aureus* can not only degrade the antibacterial triglycerides secreted by human skin,[57] but the hydrolysate can also acidify the protective skin, thus promoting deep invasion.[58] Similarly, the high level of hyaluronidase (HAase) produced by some bacteria can damage the connective tissue and help establish infections.[59] Therefore, the bacteria-secreted enzymes can be recognized as specific triggers to activate responsive materials for bacterial-targeting killing. And the rationale behind it is primarily the enzyme-triggered release of antibacterial agents, which can be divided into two strategies: (1) enzyme-induced cleavage of the linkage between drugs and carriers; and (2) enzyme-induced destruction of the encapsulating materials. The designs will be introduced below in terms of the enzyme category.

2.2.1 Lipase. Since the development of Ring-Opening Polymerization of ε-caprolactone in the early 1930s,[60] the product poly(ε-caprolactone) (PCL) has been investigated as a biocompatible polymer, and its lipase-degradable property has been widely studied over the years.[61,62] Exploiting the lipase-sensitive property of PCL, Wang *et al.* developed a reverse micelle (RM) based on quaternary ammonium groups (QPs) named as QP-*b*-PCL-*b*-QPs, formed by self-assembly of the triblock copolymers in tetrahydrofuran (THF). The bactericidal QPs were at both ends of the polymer chain and were kept in the core of the micelle, while PCL was in the shell resulting from its hydrophobicity, as shown in Fig. 3A. Benefiting from the biocompatibility of the PCL shell of the micelle, the RM demonstrated a minimal toxicity towards mammalian cells. Moreover, the PCL moiety could be hydrolyzed by bacterial lipase, resulting in the exposition of biocidal quaternary ammonium functionalities and the elimination pathogens.[63] Another approach for PCL-based activation is so-called "caging" strategy. In this case, PCL-containing anionic polymer could be used to neutralize the positive charge toxic cationic agents, whose antimicrobial activity could only be recovered once the PCL is degraded to remove the "cage" by lipase. Accordingly, cationic poly(2-(methylamino)ethyl methacrylate) (PDMA)[64] and Ga^{3+} ions[65] were used in this strategy, respectively, exhibiting lipase-responsive release of cargos. In addition to PCL, fatty acid esters are the natural substrate of lipase, and the derived materials have also been utilized as lipase-sensitive carriers for the delivery of antibiotics. For example, a biomimetic vitamin-based lipid (ascorbyl tocopherol succinate, ATS) was reported to possess a 35-fold stronger binding affinity to lipase than its natural substrate, as analyzed *in silico*. The ATS could be cleaved by lipase and release the vancomycin that loaded in the ATS-based solid lipid nanoparticles (VM-ATS-SLN).[66] Likewise, a liposome shell could be degraded by bacterial lipase, and the biocidal cargo, colistin-loaded mesoporous silica core (Col@MSN), could be released.[67]

2.2.2 Hyaluronidase. HAase is a type of endoglycosidase that can cleave the glucosidic bonds within the polysaccharide hyaluronic acid (HA), and breaks down HA into monosaccharides.[68] HA, a negatively charged natural extracellular matrix (ECM) component, is known as non-toxic and biodegradable, rendering it an ideal responsive carrier for bactericidal agents.[69] A popular strategy is based on HA-modified surfaces for selective release of cargos and the antibacterial coatings where HA was externally exposed. In the case of a chitosan–silver nanocomposites (Chi@Ag NPs)/HA composite coating prepared by layer-by-layer (LBL) self-assembly, due to the degradation of HA by bacteria-produced HAase, the Chi@Ag NPs/HA composite coating became unstable. As a result, Ag NPs and the corresponding Ag^+ ion could be released to kill bacteria without damaging surrounding environment.[70] The same LBL approach was also used to prepare (1) vancomycin (Van)-loaded Chi/HA multilayers,[71] and (2) HA-gentamicin (GEN) conjugated (HA-Gen)/Chi polyelectrolyte multilayers.[72] On-demand release of Van or Gen can be achieved through the degradation of the conjugated HA by HAase. By applying another pH-sensitive module, the HA-based coating could perform as a dual-responsive design as well. Polyacrylic acid (PAA)-chitosan quaternary ammonium salt (QCS) assembly

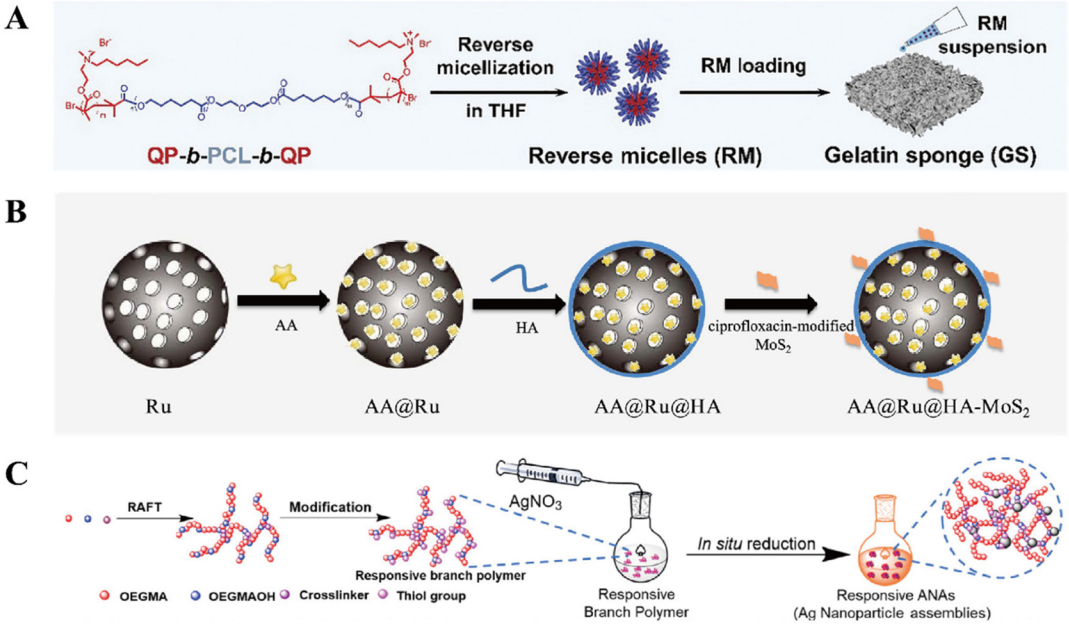

Fig. 3 (A) Schematic illustrations of the lipase-sensitive QP-*b*-PCL-QPs reverse micelles. Reprinted with permission from ref. 63. Copyright 2021, Wiley-VCH. (B) HAase-responsive nanosystem AA@Ru@HA-MoS_2. Reprinted with permission from ref. 74. Copyright 2019, American Chemical Society. (C) Schematic illustrations of SlplB-responsive ANAs. Reprinted with permission from ref. 80. Copyright 2020, American Chemical Society.

could be coated by HA, upon degradation of HA outer layer and pH-mediated decrease of electrostatic interaction between PAA and QCS, biocidal QCS was released.[69] Other than coatings on the macroscopical surface on the material, HA was also used for microcosmical coating on nanoparticles.[73,74] For example, ascorbic acid (AA)-loaded mesoporous Ruthenium (Ru) nanoparticles can be encapsulated in HA, followed by further surface modification to introduce MoS_2 content, giving rise to an antibacterial nanosystem AA@Ru@HA-MoS_2, as shown in Fig. 3B.[74] After the capping HA being decomposed by HAase at infectious sites, AA was released and catalyzed by MoS_2 to generate bactericidal $^{\bullet}OH$.

2.2.3 Other enzymes. Alkaline phosphatase (ALP) is an enzyme found in many microorganisms which can catalyze the hydrolysis of not only monoesters of phosphoric acid,[75] but also polyphosphoesters (PPEs) under physiological conditions.[76] In this approach, a chitosan membrane consisting of PPEs and minocycline hydrochloride (PPEM) was developed and demonstrated excellent antibacterial activity. The PPEs served as crosslinkers in the membrane, and thereby upon the phosphate being cleaved by the overexpressed ALP at the infection site, the PPEM could be liberated from the membrane and then killed the bacteria.[76] Furthermore, by integrating carboxylic esters and phosphoesters in a single polymer chain, the materials can be endowed with dual-responsiveness to lipase and ALP.[77] A mannose-grafted copolymer Man-*g*-P(EPE-*r*-TPE)-based nanoparticle (mPET) was designed to this end, where EPE contained phosphate esters and TPE contained carboxyl esters. It was used to encapsulate the ciprofloxacin-deferoxamine complex (DFO-CIP) to obtain mPET@D_{Fe}C nanoparticles, which could release the antibacterial DFO-CIP when encountering ALP and lipase. Serine protease-like protease B (SplB) is a protease as well as a virulence factor secreted by *S. aureus*.[78] Through rational integration of the peptide sequence that can be recognized and cleaved specifically by SplB into drug carriers, SplB-controlled antibiotic release can be realized. The oligopeptide GSWELQGSGSC, with the enzymatic site located between Q-G, is one of the SplB-cleavable sequences.[79] In an implant coating (Ti-SPR-Van) reported recently, one end of this peptide was linked on the Titanium (Ti) implant surface, while the other end was conjugated with an antibiotic, vancomycin. The hydrolysis of Ti-SPR-Van by SplB was evidenced *via* the appearance of the peak of the cleaved product (Van-GSWELQ) in MALDI-TOF-MS (matrix-assisted laser desorption/ionization-time of flight mass spectrometry) analysis.[79] WELQK is another SplB-sensitive peptide sequence, based on which Zuo *et al.* developed Ag nanoparticle assemblies (ANAs) with WELQK-containing branched copolymers as crosslinkers (Fig. 3C).[80] The ANAs underwent a stable/collapsed transition when exposed to SplB, and Ag^{+} released from the collapsed ANAs exhibited biocidal activity to MRSA. Other enzymes such as glutamyl endonuclease (V8 enzyme),[81] type IV collagenases,[82] and β-lactamases[83] have also been reported as triggers for antibiotic release. In summary, these enzyme-responsive platforms achieved on-demand antibiotics release and demonstrated good antibacterial efficacy at the infection site.

2.3 Reactive oxygen species (ROS)

ROS is a kind of oxygen-containing unstable molecule, including superoxide anion (O_2^{-}), hydrogen peroxide (H_2O_2),

hydroxyl radical ($^{\bullet}OH$), and singlet oxygen ($^1O_2$), all of which are known as deadly weapons of the immune system against pathogen infections. Innate immune cells, such as phagocytes and neutrophils, are recruited by infection-induced inflammation, subsequently generating high level of ROS to eliminate microbes by oxidative damage of cellular components.[84] Thus, the rational exploration of the aberrant level of ROS can realize the controllable release of antimicrobial cargos to treat an infection.

Boronic acid (R-B$(OH)_2$) is a kind of Lewis acid that can be reversibly conjugated to the diol-containing substance to form the ROS-sensitive borate ester bonds, based on a fact that ROS can act as nucleophilic reagents to react with the borate ester and cleave it.[85] Borate ester segment can be incorporated in drug-loading hydrogel by either as a built-in crosslinker or pending monomeric unites, thus enabling ROS-responsive delivery.[86–90] For example, as illustrated in Fig. 4, a ROS-sensitive gel was prepared by crosslinking poly(vinyl alcohol) (PVA) utilizing a bifunctional phenylboronic acid linker.[86] An antibiotic clindamycin (CDM) was encapsulated inside the hydrogel, which was further deposited on a microneedle to promote skin penetration. The hydrogel underwent rapid degradation when exposed to 1 mM H_2O_2 *in vitro*, stemming from the cleavage of borate ester crosslinker by the ROS, while it was stable in the absence of H_2O_2. Subsequently, the sustained release of the entrapped CDM from the degraded gel was detected. In addition to hydrogels, borate ester-based micelle has also been developed for the controlled release of antibacterial payloads. For example, 4-(hydroxymethyl) phenylboronic acid pinacol ester (HPAP)-modified cyclodextrin (Oxi-αCD) was used as a carrier to entrap antibiotic moxifloxacin (MXF) to prepare nanoparticles (MXF/Oxi-αCD NPs), which could be oxidized and degraded by H_2O_2, thus releasing the MXF.[91] In another work, phenylboronic acid pinacol ester-containing copolymer was used as a hydrophobic block to prepare micelle with PEG for the ROS-triggered release of the encapsulated rifampin.[92]

Thioketal (TK, –SC$(CH_3)_2$S–), a sulfur analog of ketal, is another attractive linkage that is cleavable by ROS. TK is generally stable in enzyme-rich and acidic or basic environments, whereas it readily breaks into non-toxic thiol and acetone products when exposed to ROS.[93] In a ROS-responsive nanoparticle system, a TK-conjugated PEG (mPEG-TK) was linked to the surface of vancomycin-loaded mesoporous silica nanoparticles (MSNs).[94] Upon the interaction with ROS at the infection site, mPEG-TK on MSNs surface was degraded, subsequently, the loaded Van escaped. Furthermore, the diselenide bond (–Se–Se–) is also one of the ROS-sensitive linkages, which is believed to be hydrolytically stable in physiological conditions, offering advantages over ester bonds. The diselenide bond has a low dissociation energy of about 176 kJ mol^{-1}, which makes it easily to be oxidized and cleaved in the presence of oxidative stress.[95] Thus, by integrating diselenide into drug carriers, the ROS-triggered release of antibiotics can be realized.[96] Last but not least, keratin, a protein widely used in biocompatible hydrogels, is reported as multi-stimuli-responsive, owning to its abundant disulfides (–S–S–) and amino acids. The disulfide within keratin can be oxidized to the easily dissolved thiosulfinate (–S–SO–) or thiosulfonate (–S–SO_2–), endowing the keratin-containing hydrogel with a ROS concentration-dependent degradation feature for the pathological ROS-induced release of the loaded antimicrobial agents.[97]

2.4 Other intrinsic stimuli

Other promising intrinsic stimuli that are not classified into the above categories include glutathione (GSH), salt, and toxin. GSH is a tripeptide produced by both mammalian cells and prokaryotes. As ROS can oxidize the cysteine's sulfhydryl

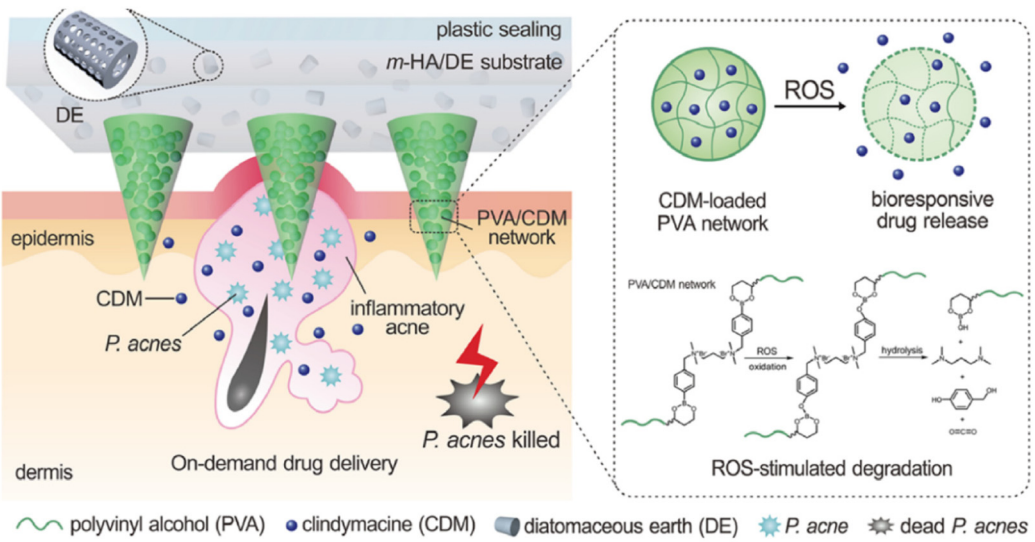

Fig. 4 Schematic illustration of the ROS-responsive delivery of CDM by boronic ester-based structure in the microneedle. Reprinted with permission from ref. 86. Copyright 2018, Wiley-VCH.

bond, many bacteria produce GSH to combat oxidative stress.[98] Hence, the reductive GSH can act as a trigger to cleave redox-sensitive bonds, such as disulfide bonds in the encapsulating materials, and then boost the release of the loaded antibiotics.[99] Another tactic taking advantage of the redox reductive infection microenvironment is through GHS-mediated redox reaction of metal. The hexavalent tungsten, W(VI), in tungsten-polyoxometalate clusters (POMs) could be reduced by reductive ROS in biofilm microenvironment to pentavalent tungsten, W(V). This transformation significantly improved the photothermal conversion of the materials and consequently enhanced the bacteria-killing efficacy.[100] In addition, salt-responsive fabrics have achieved the feature of bacterial killing and the releasing of dead bacteria in response to the switch between water and salt solution due to the ionization and deionization of zwitterionic polymers.[101–105] Certain toxins, such as the α-toxin elaborated by *S. aureus* to disrupt cellular membranes, can function as pore formers on liposomes to trigger the release of the antibacterial cargos.[106]

3. Extrinsic stimuli

Albeit numerous endogenous stimuli-responsive materials have been developed, it remains challenging to achieve precisely controlled antibacterial behavior because of the intricate environment in the body and the unpredictable inter-individual diversity.[107] Hence, exogenous stimuli-activated platforms are considered beneficial as these stimuli can be manipulated easily and accurately. The extrinsically responsive materials are sensitive to external triggers, such as light, temperature, electromagnetic fields. Elaboratively designed extrinsic stimuli-responsive antibacterial materials and the mechanism of action are discussed in this section.

3.1 Light

Light is considered non-invasive to a certain degree and can induce photochemical reaction without the change in other parameters,[108] and it can be imposed directly with spatiotemporal accuracy. Photo-responsive materials are also less likely to cause AMR owing to their mode of action,[109] which will be elucidated below. Typically, light-responsive materials towards antibacterial applications primarily involve two strategies: antimicrobial photothermal therapy (aPTT) and antimicrobial photodynamic therapy (aPDT).

3.1.1 aPTT. The aPTT is a technique in which photosensitizers are exploited as photothermal agents (PTAs) to convert electromagnetic radiation to heat to kill pathogenic bacteria. Since the localized hyperthermia generated by the PTAs kills bacteria by impairing the bacterial structure and damaging the membrane permeability which does not rely on the bacterial metabolic pathways, the antibacterial spectrum of aPTT is broad, and the development of AMR is scarcely possible. Compared to ultraviolet and visible light, near-infrared (NIR) light with wavelengths 700–1300 nm can penetrate skin and tissue deeply, with minor damage to the surrounding healthy tissues.[110] Consequently, the NIR-triggered photothermal conversion received great interests, and considerable efforts have recently been made to develop the novel NIR-responsive PTAs for aPTT based on noble metals[111,112] and other transition metal[113–115] and organic[116,117] systems.

Under photo-excitation, localized surface-plasmon resonance (LSPR) of noble metal-based nanoscale PTAs leads to collective oscillation of free electrons, which induces the non-radiative relaxation and generates localized hyperthermia.[118] For example, gold-silver nanocages (Au–Ag NCs) have evoked extensive attention as their LSPR absorption is tunable by changing the Au/Ag ratio. The hyperthermia generated by the LSPR and the bactericidal Ag^+ released from the NCs can create a synergistic antibacterial therapy. In particular, applying a mesoporous silica coating on the surface of the NCs achieved the sustained release of Ag^+. The temperature of the fabricated Au–Ag@SiO_2 NCs solution rose to 54.7 °C after 10 minutes of 808 nm irradiation, and the Ag^+ release was verified by inductively coupled plasma mass spectrometry (ICP-MS), which led to excellent bacterial killing efficacy.[112]

MoS_2 nanosheets, a typical transition metal sulfides (TMS) material, have shown excellent photothermal conversion efficiency under 808 nm irradiation. Since PTAs can be switched from ground state to excited state and relax to ground state with energy dissipation in the form of heat, the narrow band gap of 1.8 eV for MoS_2 indicates the high photothermal conversion efficacy of this nanomaterial in the NIR spectral range.[119,120] By introducing another PTA, polydopamine (PDA), into the MoS_2 nanosheets through the coordination between MoS_2 and catechol groups in dopamine, the photothermal property of the nanomaterial can be even further enhanced. In a MoS_2-PDA nanozyme-loaded hydrogel (MPH) system, the absolute value of temperature rise and bacterial killing efficacy after continuous 808 nm irradiation are both higher than the control group without PDA, indicating the introduction of PDA into MoS_2 nanosheets can effectively improve the photothermal and antibacterial performance of MoS_2 nanosheets.[115]

Organic PTAs also have received much interests due to their decent degradability and biocompatibility.[121] However, the complicated design as well as synthesis, and the limitation in absorption wavelength have impeded the development of organic PTAs.[122] One strategy used recently to address this problem is the modification of the charge-transfer complex (CTC), in which the charge can transfer from the electron donors to the acceptors thus causing the electron delocalization between donors and acceptors. The HOMO–LUMO energy gap of this conjugated system can be reduced to achieve a better photothermal conversion if the electrons of acceptors are delocalized by increasing the π-electron donating ability of donors. The narrowed energy gap of CTCs amplifies the NIR-light absorption and consequently enhances the non-radiative transition to generate hyperpyrexia.[123,124] In this case, Tian *et al.* reported for the first time the fabrication of CTC nanoparticles with absorption peak in NIR-II region, by combining the commercially available donor, perylene (PER), and accep-

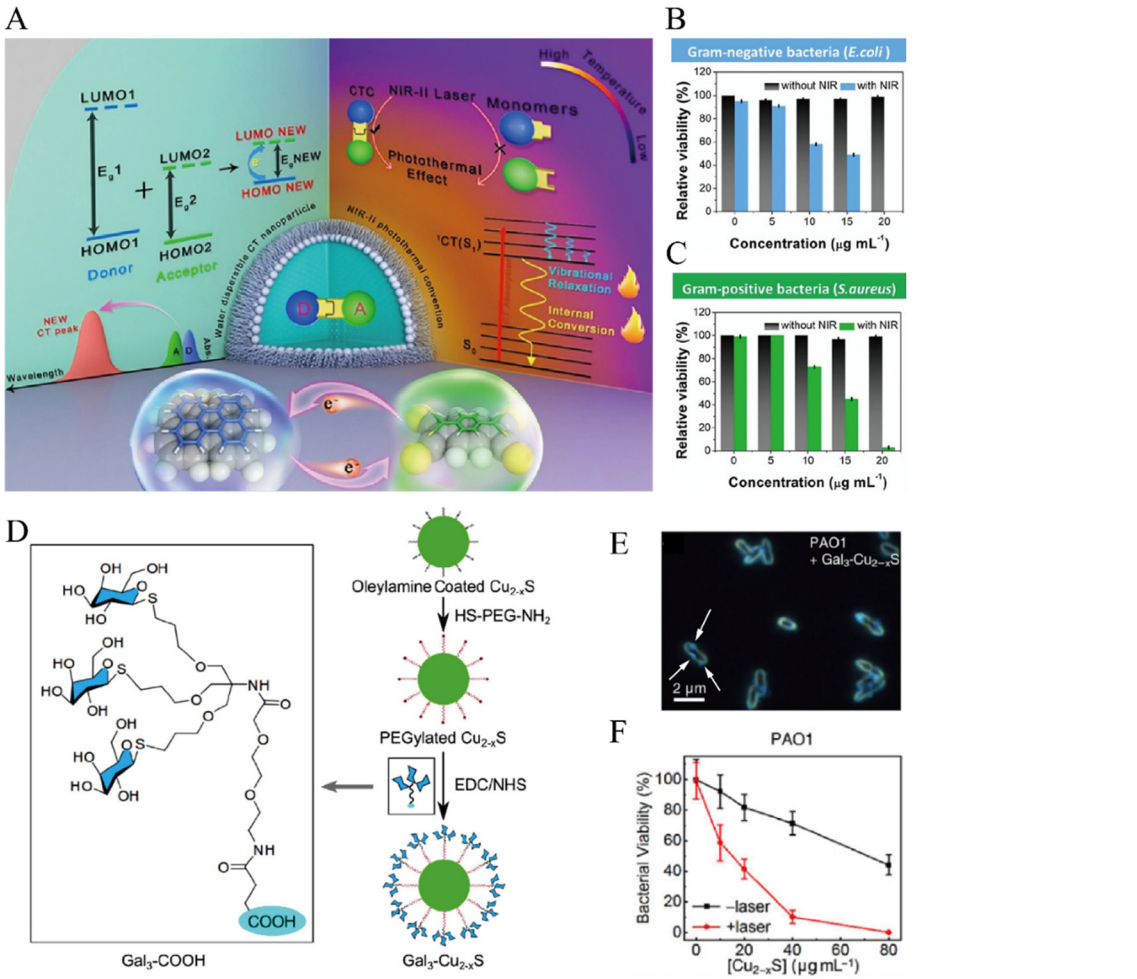

Fig. 5 (A) Diagram showing photothermal effect in charge transfer cocrystal nanoparticle and its *in vitro* antibacterial efficacy against Gram-negative bacteria *E. coli* (B) and Gram-positive bacteria *S. aureus* (C). Reprinted with permission from ref. 116. Copyright 2021, Wiley-VCH. (D) Illustration of the active targeting galactosylated Cu_{2-x} S NCs. (E) The binding between Gal_3-Cu_{2-x} S and PAO1 in dark-field microscopy. (F) Killing of PAO1 by the Gal_3-Cu_{2-x}S NC with and without laser irradiation. Reproduced with permission from ref. 137. Copyright 2019, Wiley-VCH.

tor tetracyanoquinodimethane (TCNQ) (Fig. 5A).[116] The photothermal conversion efficiency of PER-TCNQ NPs was calculated to be 42% and was comparable to the state-of-the-art NIR-II PTAs materials, which endowed PER-TCNQ NPs with remarkable bactericidal activity for both Gram-negative and Gram-positive bacteria (Fig. 5B and C).

3.1.2 aPDT. The aPDT is a clinically approved technique, in which photosensitizers (PS) are used to generate bactericidal ROS. Generally, upon light irradiation with a given wavelength, the PSs can be excited from the ground state to the triplet excited state, and transfer electrons to molecular oxygen to produce O^{2-} and $^{\bullet}OH$, or transfer the energy to triplet state oxygen to create $^1O_2$, subsequently giving rise to the mass production of ROS.[125] Apart from directly disrupting the bacterial structure to kill pathogens by oxidative damage, ROS can also induce indirect killing including proteolytic elimination and autophagy, *etc.*,[84] this mechanism also eliminates the chance of developing AMR. Both inorganic metal-based and organic PSs have been developed lately for aPDT.

TiO_2 can be stimulated by UV light, where the electrons in the valence band are excited to the conduction band while leaving an electron–hole in the valence band, thereby generating ROS.[126] By modifying noble metal nanoparticles on TiO_2, its photocatalytic efficiency can be extended from UV to the visible and NIR spectral range, benefiting from the light harvester and sensitizer properties of plasmonic nanostructures. Marín-Caba *et al.* fabricated an Au nanorod (AuNR)-modified TiO_2-based plasmonic photocatalytic hybrid composite for solar-light sensitive antibacterial coating.[127] The AuNR enhanced the photosensitization of TiO_2 by both the direct electron transfer effect and the intense local fields around the tips of the nanorods.[128] When exposed to a solar simulator with wavelength 350–2400 nm, the nanocomposites produced suffice $^{\bullet}OH$ and $^1O_2$ to eliminate the *E. coli* grown on the nanocomposite film.

Chlorin e6 (Ce6), one of the most widely used organic PSs, is a second-generation PS featured with high sensitizing efficacy and low dark toxicity.[129] An antibacterial and anti-

cancer multifunctional gelation system was developed by introducing Ce6 into a silk fibroin (SF)-based hydrogel (SFMA-Ce6). Under the irradiation of 660 nm light with 20 mW cm^{-2}, ROS produced by SFMA-Ce6 was validated by a commercial singlet oxygen fluorescence probe and was confirmed to be sufficient to suppress melanoma and facilitate the recovery of *S. aureus* infected skin.[130] Albeit great success has been achieved for aPDT in the broad-spectrum killing, selective obliteration of bacteria is also of great interest to avert microbiota imbalance.[131] To this end, α-D-galactose (αGal) and rose bengal (RB)-contained monomer were copolymerized by reversible addition–fragmentation chain transfer (RAFT) polymerization to obtain water-soluble PαGal_{50}-*b*-PGRB_n, a diblock copolymer can self-assemble into micelles with αGal corona.[132] It is noteworthy that the αGal can specifically bind to LecA, a galactose-specific lectin produced by *P. aeruginosa*. Therefore, the ROS generated by the RB PSs with a short diffusion distance and a short half-life could realize a selectively killing of the bacteria.

As ROS could enhance the thermal sensitivity of bacterial membrane, aPDT has been implemented simultaneously with aPTT to overcome the limitation of aPTT. The hyperthermia generated during aPTT might cause damages to healthy tissues. With the combination of aPDT, a lower temperature could be bactericidal while avoiding damaging normal tissues.[110] Also, mild thermal therapy could increase the permeability of the bacterial membrane, thereby promoting the intracellular uptake of ROS.[121] Hence, the synergistic therapy of aPDT and aPTT could boost the therapeutic efficacy compared to a single treatment and has been extensively studied in recent years.[25,133–136] Hou *et al.* galactosylated the copper sulfide nanocrystals (Cu_{2-x} S NCs), a successful photo-agent for combined PTT and PDT, to target LecA expressed on the surface of *P. aeruginosa* PAO1 (Fig. 5D).[137] The resulting Gal_3-$Cu_{2-x}S$ could bind to the surface of PAO1, as demonstrated by the blue scattering light from $Cu_{2-x}S$ NC surrounding the bacteria contour under dark-field microscopy (Fig. 5E). This binding is believed to reduce the concentration of NCs needed to kill the pathogens because of the shortened distance between the generated ROS and bacterial cells. And an *in vitro* killing rate of 100% was achieved upon NIR-light irradiation of 1064 nm (1 W cm^{-2}, 10 min) at a higher concentration they tested (Fig. 5F).

3.1.3 Other light-responsive systems. Although aPDT and aPTT are the most widely applied strategies in photo-triggerd antibacterial therapy, other promising approaches are also under intense research and development. Wei *et al.* reported a smart supramolecular antibacterial surface that can switch its biocidal property to bacteria-releasing activity upon UV light irradiation.[138] This function was endowed by a light-responsive molecule azobenzene (Azo), whose trans-structure can form stable complex with a host molecule cyclodextrin (CD), whereas the *cis*-Azo transformed by UV light could not fit in the CD cavity because of the size mismatch. A quaternary ammonium salt (QAS)-containing CD was used as a bactericidal agent which was incorporated on the Azo-containing surface by host–guest interaction between CD and Azo, and it could effectively kill the attached bacteria. Upon UV radiation, the CD-QAS/Azo complex dissociated to remove the dead bacteria from the surface. And the original surface could be regenerated by the exposure of visible light and the addition of CD-QAS. Similar strategy was reported where light-responsive 4,5-dimethoxy-2-nitrobenzyl group underwent photolysis reaction to shift a cationic polymer hydrogel surface to zwitterionic. The latter form was antifouling and could release the dead bacteria killed by the cations.[139]

3.2 Temperature

The difference in temperature before and after heat generation from PAs could activate the antibacterial performance of thermo-responsive materials, as the properties of this kind of materials can be abruptly altered within a slight change in the ambient temperature.[108] For example, poly(*N*-isopropylacrylamide) (pNIPAM), one of the most commonly studied thermally responsive polymer, can undergo a conformational change (expanded to collapsed) when the surrounding temperature cross above its lower critical solution temperature (LCST) as a result of a hydrophilic to hydrophobic transition,[140] which is considered as an intramolecular first-order phase transition.[141] For the convenience of discussion, we classify temperature as an exogenous stimulus, but it should be noted that this kind of material can be designed to respond to either endogenous or exogenous factors-induced temperature changes. Typically, the strategies for temperature responsiveness can be factored into two categories based on their working mechanisms, namely, the release of loaded antibiotics and the repulsion of bacterial adhesion.

3.2.1 Temperature-induce drug release. The primary means for the drug release from the thermo-responsive delivery system is through the structural destruction of the drug carriers. In a temperature-sensitive polymer network, such as hydrogels and polymer films, the network is swollen below the LCST of the constructing polymers, but as the temperature elevated above the LCST, the structure of the gels or films could collapse induced by their increasing hydrophobicity upon the coil-globule transition. Consequently, when the hydrogels or the films shrank, the encapsulated antibiotics were extruded into the surroundings.[142–144] In addition to the collapsing mode, a higher temperature could also break the ionic complexation that formed the hydrogel. An exemplary hydrogel dressing with antibacterial capability was crosslinked by the complexation between the hydroxy group in carboxymethyl agarose (CMA) and Ag^+, the amount of bactericidal Ag^+ released was elevated with increasing temperature, which disrupted the crosslinking.[145] Furthermore, some materials have relatively low phase transition points that can be exploited for drug carriers, as these materials were converted into liquids when the temperature was heated above the melting point, thus releasing the encapsulated drugs.[146,147] Qing *et al.* developed a thermo-responsive drug-delivery nano-transporter (TRIDENT) consisting of the natural fatty acids-based nanoparticle with a melting point of 43 °C, a broad-spectrum antibiotic imipenem (IMP), and a photothermal agent IR780.

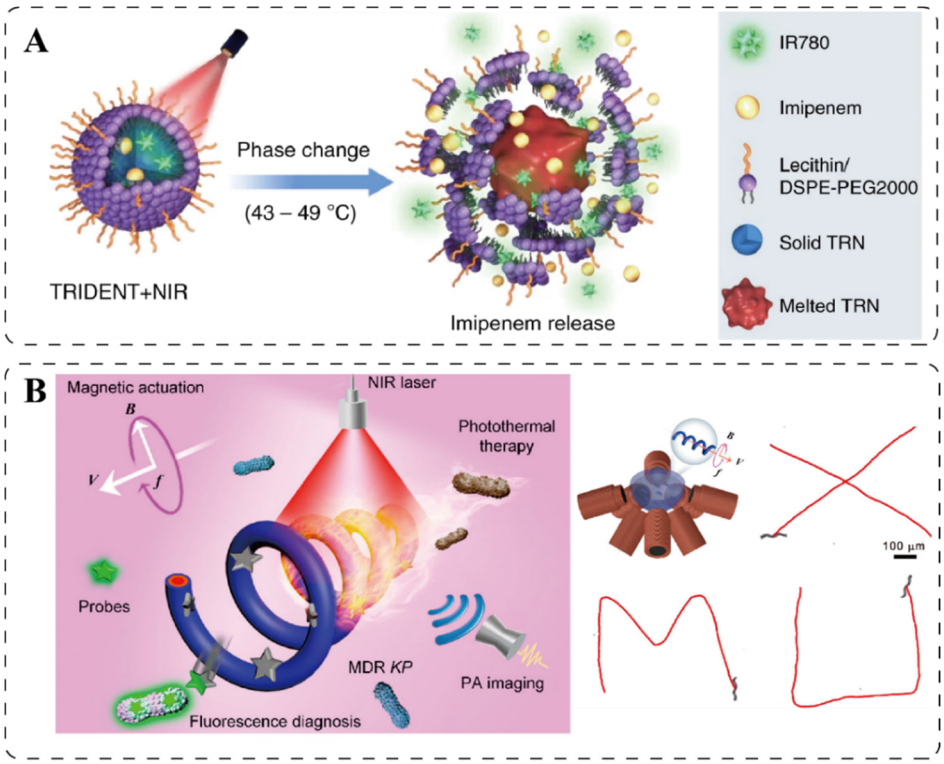

Fig. 6 (A). Antibiotic IMP releasing from the temperature-responsive TRIDENT due to the melting of drug-loaded TRNs. Reprinted with permission from ref. 146. Copyright 2019, Nature. (B). Schematic illustration of the MSP nanoswimmer and its controlled motion trajectories under magnetic field guidance. Reprinted with permission from ref. 152. Copyright 2020, American Chemical Society.

Upon the temperature rising to above 43 °C under NIR irradiation, the thermal-responsive nanostructure was melted, accompanied by a reduction in size and the release of loaded IMP, as shown in Fig. 6A.[146]

3.2.2 Switchable bacterial killing and release. The temperature-responsive materials are also used in the "kill-and-release" strategy. Traditional antibacterial surfaces are either passively defensive to prevent bacteria adhesion or actively attack to kill the attached bacteria. Though effective, the former cannot remove the pathogens after they adhere, and the latter often suffers from the accumulation of dead bacteria.[148] Therefore, the kill-and-release mechanism was proposed, in which the smart materials can kill the adhered bacteria, and release the dead ones and the debris to re-expose the clean active surface triggered by the stimuli of choice. As pNIPAM experiences the hydrophilic–hydrophobic transition at LCST, the pNIPAM-containing surface can be switched from bactericidal to bacteria-repellent to release the dead bacteria and debris, when the temperature decreases[149,150] In addition, the thermos-responsive property of pNIPAM can be further combined with photo-thermal conversion, in which the heat generated by PTAs triggers the change of bio-interfaces. Wang *et al.* developed an antibacterial surface which was composed of tannic acid and Fe^{3+} ions coordination complex as PTAs, and grafted pNIPAM as thermos-responsive moiety. Both attached Gram-positive (*i.e.*, MRSA) and Gram-negative bacteria (*i.e.*, *E. coli*) can be killed by the localized hyperthermia produced by the TA/Fe complex. And more than 90% of bacteria were removed from the surfaces when they were placed in 4 °C after the aPTT to allow the cooling and consequently the switch of surface wettability.[151] This self-clearance strategy addressed the problem of traditional aPTT surfaces, in which remaining dead bacteria served as both proinflammatory factors and nutrient of other bacteria.

3.3 Magnetic field

Externally imposed magnetic fields can manipulate the movement of magnetic nanoparticles (MNPs) and the transformation of the morphology of MNP-based assemblies. Similar to the aPTT, the MNPs can respond to the magnetic fields to generate heat for direct thermal-killing of bacteria or the release of drugs, which will be discussed in the following parts.

Bacteria in biofilms are protected by the self-produced extracellular polymeric substances (EPS), which hinders the penetration of many antibiotics. To promote the entrance of therapeutic agents into the biofilm, the MNPs-based antibacterial materials can be navigated by magnetic fields to penetrate through the biofilm, benefiting from their superparamagnetic property. Fe_3O_4 nanoparticles are widely used for this purpose.[73,152,153] For example, Xie *et al.* reported a Fe_3O_4-magnetized *Spirulina* (MSP) microswimmer capable of con-

trolled locomotion and multiagent propulsion.[152] This helical microrobot performed a corkscrew motion for propulsion under the magnetic field generated by electromagnetic coil pairs, and successful propulsion along the trajectories of uppercase letters "XMU" was captured, as shown in Fig. 6B. Through the photosensitizer polydopamine that was *in situ* polymerized on the MSP microswimmer, the aPTT was applied to kill the multidrug-resistant *Klebsiella pneumoniae* (MDR KP) inside the biofilm. Another approach for the antibacterial agents to penetrate the biofilm is by imparting a physical force by magnetically transformed sharp edges to disrupt the dense EPS. Graphene oxide (GO) is a 2D nanomaterial that can align in different orientations in a magnetic field, as the aromatic rings in GO can overcome the thermal disordering effects. The direction of the GO greatly influences the insertion angle and its sharp-edge density in contact with the bacterial membrane. Namely, vertically oriented GO nanosheets exhibited higher antimicrobial activity than random or horizontal orientations due to an increased density of sharp edges.[154,155] Likewise, magnetic Galinstan-based liquid-metal microparticles also showed a distinct difference before and after magnetization, as in response to rotating magnetic fields, the particles transformed from spheres to 3D extruded particles, including jagged spheres, nanorods, and nanostars, whose sharp edges induced physical damages to the mature biofilm.[156]

The alternating current magnetic field can realize the heating of biological tissue through MNPs, originating from the coupling of the atomic magnetic moments to the crystal lattice in these materials.[157] Fe-based MNPs are commonly exploited in this regard.[158–160] Hou *et al.* fabricated the Janus magnetic nanoparticles Au/$MnFe_2O_4$ (Au/MFO) consisting of a 9 nm tetrazine (Tz)-modified Au component for active targeting of bacteria and a 15 nm $MnFe_2O_4$ component for the magnetic-thermal killing of bacteria.[160] The Tz group in Au/MFO could selectively reacted with the *trans*-cyclooctene (TCO) group anchored on the cell wall of Gram-positive bacteria by a click-type bioorthogonal reaction. Upon attaching to the bacterial cell wall, the Au/MFO nanoparticle generated localized hyperpyrexia and obliterated bacteria in an alternating magnetic field (400 A, 30 min). Furthermore, the heat produced under alternating magnetic field (AMF) can also trigger the release of drugs encapsulated in core@shell MNPs for antibacterial application. For example, the cucurbit[6]uril (CB[6]) capped on MNPs-containing MSNs can act as thermosensitive gatekeeper that can detach from the MSNs when the particles were heated by AMF due to a decrease in the binding constant in response to an increased temperature.[161] Subsequently, the drugs loaded in MSNs, ranging from the large-molecular-weight and positively charged AMPs to the small-molecular-weight and negatively charged antibiotics, can be released to eradicate pathogenic biofilms.[162]

3.4 Other extrinsic stimuli

Ultrasound (US), electrical current, and mechanical force that do not fall into the abovementioned categories are also effective extrinsic stimuli for antibacterial applications. Since US with a low tissue attenuation coefficient can penetrate deep inside the human body without causing tissue damage.[163] Therefore, US-based antibacterial sonodynamic therapy (aSDT) is considered a promising alternative to aPDT, aiming to overcome the low penetration of external light. Under the high-intensity ultrasound, the sonosensitizers (SSs) can generate ROS to eliminate bacteria. Although the mechanism of ROS generation is still not utterly clear and is believed to be multifaceted, two main mechanisms have been proposed.[164] The first relies on sonoluminescence, a process in which light can be produced under ultrasound irradiation. The generated light can activate the sensitizers to produce ROS in a similar manner to PDT. The second proposed mechanism is based on pyrolysis, in which the temperature elevation by inertial cavitation could break down the sensitizers to generate ROS.[165] Several PSs can also be used as SSs for antibiosis, among which the porphyrin derivatives[166–168] and porphyrin-like materials[169] are broadly studied. Under US irradiation, the porphyrin can be transformed from ground state to excited state, then relax to the triplet state and transfer electrons to molecular oxygen to produce ROS. It has been reported that introducing porphyrin as a ligand of a metal–organic framework (MOF) HNTM could improve the stability of porphyrin. Doping of platinum (Pt) atoms into the HNTM to form HNTM-Pt can enhance the SDT efficacy, as the Pt atoms have strong oxygen absorption so that more O_2 can be absorbed to the SSs to produce ROS. Furthermore, loading AuNRs into HNTM-Pt could further improve the SDT performance by increasing US cavitation (Fig. 7A).[166] Different from the porphyrin-based materials, the generation of ROS from the metal-based SSs mainly relies on the shifting of excited electrons from the valence band to the conduction band, which induces the separation of electrons and holes, consequently the reaction with oxygen. In this regard, copper-containing SSs, such as CuS[170] and Cu_2O,[170] are exploited for aSDT.

Electrical stimulation is also an attractive trigger benefiting from its high level of spatio-temporal controllability and biocombatibility.[171,172] The electricity-responsive property can be embedded in flexible electronic devices for antibacterial applications. One effective strategy is through electrochemiluminescence (ECL)-based antibacterial electroluminodynamic therapy (ELDT). When applying a voltage to the ECL system, ECL reagents can emit light, which can be absorbed by a matched PS to produce bactericidal ROS. For example, luminol (5-amino-2,3-dihydro-1,4-phthalazinedione) in a flexible hydrogel emitted light with a wavelength of 400–500 nm on the surface of a glassy carbon electrode when applying the voltage with a potential region from 0.2 to 0.6 V at a scan rate of 100 mV s^{-1}. This ECL occurred during relaxation from the excited state to the ground state of the reactive intermediate produced by the anodic oxidation of luminol. A cationic PS, oligo (*p*-phenylenevinylene) (OPV), with a broad absorption in the region of 350–500 nm, was used to transfer the absorbed energy to the surrounding oxygen molecules to generate ROS (Fig. 7B). The cationic OPV could bind to the negatively charged bacterial surface and kill the pathogenic bacteria sim-

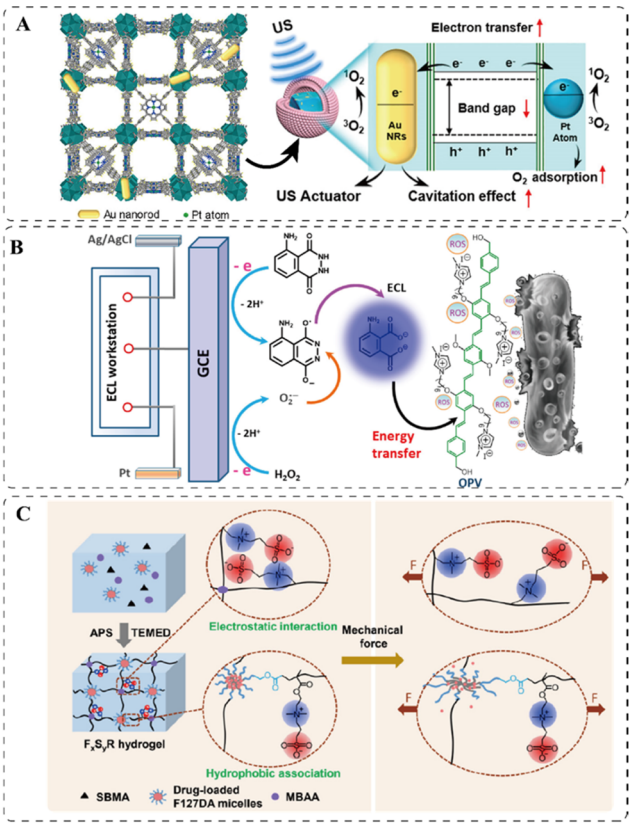

Fig. 7 (A) 3D structure of the sono-responsive HNTM-Pt@AuNRs and its proposed mechanism of ROS generation. Reprinted with permission from ref. 166. Copyright 2021, American Chemical Society. (B) The electric-driven mechanism in ECL produces ROS on the electrode. Reprinted with permission from ref. 173. Copyright 2018, American Chemical Society. (C) Schematic illustration of the deformation of the mechanically responsive hydrogel under applied forces. Reprinted with permission from ref. 176. Copyright 2020, American Chemical Society.

ultaneously by ROS.[173] It is crucial for the ELDT to work that the emission spectrum of the ECL agent and the absorption spectrum of the PSs must match well. And in addition to the luminol-OPV pair, rubrene (Rub) with an emission in the range of 520–700 nm and the rose bengal (RB) PS with the absorption of 450–600 nm have also been used for efficient ELDT.[173] Other than the ELDT, the electricity-responsive materials can also undergo the electro-thermal transition to produce localized heat for effective bacterial ablation. One Ti_3C_2 MXene smart fabric showed an excellent Joule heating performance, where the heat generated by the material increased near-proportionally to the square of the input voltage, which corresponded with the Joule's law: $E = V^2t/R$, where V is the voltage, t is time, R is the resistance of the fabric, and E is the heat generated by Joule effect. Physical damages to bacteria were achieved *via* the localized temperature above 50 °C, which was easily reached by the fabric at low applied voltage.[174] Similarly, the Joule heating could also promote the release of antibiotics from a silver nanowire-based hydrogel in another work.[175]

Mechanical force is another uncommon but interesting external stimulus to activate the release of antibiotics. Fang *et al.* reported an antibacterial hydrogel, which contained Pluronic F127 diacrylate (F127DA) micelles as macro-cross-linkers and drug carriers, and the zwitterionic polymers, poly (sulfobetaine methacrylate) (polySBMA) for tissue adhesion and antifouling use.[176] The toughness of the hydrogel was determined by factors including the polymer chain entanglement, the hydrophobic association of F127DA micelles, and the electrostatic interactions of zwitterionic groups of polySBMA chains. As illustrated in Fig. 7C, when the hydrogel was subjected to either a tensile or compressive strain, the polymer chains disentangled and the hydrophobic interactions of micelles were broken, and the electrostatic interactions of polySBMA were damaged as well. All these effects lead to the deformation of the hydrogel network, thereby releasing the loaded rifampicin.

4. Application scenarios

The activatable materials can be used as therapeutics against infectious diseases or applied in medical devices to prevent contamination or treat infections. Their medical applications and their therapeutic efficacy are highlighted in this section.

4.1 Therapeutics

4.1.1 Combating the drug-resistant bacteria. Both the method of physical damage caused by external stimuli-responsive system and targeted delivery of antibiotics to the infection site enabled by internal stimuli-responsive systems can be utilized as direct therapeutics against drug-resistant bacteria. MRSA is one of the most concerning pathogens that cause nosocomial and community infections.[177] Strains resistant to broad-spectrum agents such as vancomycin have been reported.[178] In this regard, pH-induced charge reversal was combined with light-triggered aPTT to effectively treat MRSA-infected subcutaneous abscesses in mice model.[54] Acidic condition (pH 5.5) triggered Ag^+ ions release from the AgNCs[44] and vancomycin from lipid nanoparticles[40,179] promoting the healing of the MRSA-infected mice skin. In addition to MRSA, the multidrug-resistance *E. coli* (MDREC) and *K. pneumoniae* (MDR*KP*) have also become a worrying issue worldwide.[180,181] The antibiotic IMP from temperature-responsive TRIDENTs could effectively be released and stay in the infectious area, and the MDREC-infected skin could completely recover on the 15th day post-infection.[146] As the tissue damage and abscess caused by MDR*KP* infection-induced inflammation were conducive for magnetic actuation of the Fe_3O_4 MSP microswimmer. This subcutaneously injected magnetic actuation setup could promote the MDR *KP*-infected wound healing by aPTT under NIR light irradiation, as evidenced by a rapidly reduced relative infection area and the decreased bacterial colonies in the infected wound.[152]

Compared with the planktonic bacteria, the pathogens within the biofilm are more insusceptible to antibiotics and

tend to develop formidable drug resistances, as they are protected by the dense EPS.[182] To promote the penetration of antibiotics, the magnetically sensitive materials can not only be navigated into the biofilm under the guidance of magnetic fields,[73] but also form sharp ends to rip the biofilm.[156] Strong adhesion or precise delivery of antimicrobials can be achieved by the biofilm-specific microenvironment. For example, the acidic condition resulting from the anaerobic glycolysis in the EPS surrounded and anoxic biofilm promoted the charge reversal of AuNP-N-C for biofilm adhesion,[23] and lipase secreted by *Pseudomonas aeruginosa* PAO1 in the biofilm facilitated the release of toxic Ga^{3+} ions.[65]

4.1.2 Oral infection. Periodontitis is a well-known severe inflammatory disease caused by the microorganisms infection in subgingival dental plaques, which can lead to tooth loss and even systemic diseases.[183] ALP secreted by neutrophils at the infection-associated inflammatory site is a generally recognized as a biomarker of periodontal disease[184] and has been exploited as a trigger for the release of minocycline hydrochloride from an ALP-responsive drug-release membrane. The treatment with this ALP-responsive membrane effectively relieved the ligature-induced periodontitis bone loss in a mice periodontitis model, which was believed to be similar to human periodontitis, thus providing more solid support for its clinical translation.[76] Inhibiting the formation of biofilm in complicated oral environment is another challenging task stemming from the problem of both drug-resistance and patient compliance.[185] Magnetic-responsive PS-based nanoplatform was applied for the first time to treat dental caries-related biofilm, as the nanoplatform could be actuated deep inside the biofilm grew in saliva to mimic a complex environment and eliminate the bacteria by aPDT.[153] Furthermore, chlorhexidine (CHX), the "gold standard" for oral antiseptics, is suffering from the side effects of taste disturbances and teeth staining. To realize precise and controllable delivery of CHX, it was loaded in redox/pH dual sensitive Ag-decorated MSN and released in response to the pathological environment in the oral cavity. This nanocarrier exhibited little abnormal effects on the healthy mice after oral administration compared with CHX alone.[99]

Resin composite restoration is currently the most widely used treatment for dental caries, which is regarded as the most common oral disease worldwide. However, secondary caries, mainly initiated by dental biofilm, have been a huge challenge leading to the resin composite restoration failure. Liang *et al.* combined the resin dental adhesives with two tertiary amine (TA)-containing monomers, the nitrogen atoms of which could be protonated to form bactericidal QAS in response to the low pH in the infectious sites. Incorporation of TA functionalities endows resin adhesives with a long-term reversible acid-activated property, which enables a quick activation of antibacterial effect upon the protonation of TA units. Such pH-induced "on–off" switch of antibacterial activity can facilitate the achievement of anti-caries therapy while do not disturb the oral microecological balance, which has been demonstrated by using a secondary caries rat model *in vivo*.[50]

4.1.3 Bone infection. Osteomyelitis is a severe inflammatory orthopedic disease mainly caused by *S. aureus via* hematogenous spread or trauma like fracture and orthopedic surgery. The clinical treatment of osteomyelitis consists of long-term high-dose antibiotic therapy and invasive debridement, which not only have a 20% chance of treatment failure due to antibiotic resistance but also could cause tissue damage.[186] Therefore, antibiotic-free and non-invasive therapies are in need for combating against osteomyelitis. In a prototypical example, aSDT by ultrasound-sensitive materials was studied as the excellent tissue penetration of US can facilitate the treatment of deep bone infection.[166,167,169] Lin *et al.* designed the sonosensitizer protoporphyrin IX (PpIX)-encapsulated manganese oxide (MnOx) nanoparticles as the aSDT agent. It was further integrated with hybrid membrane vesicles of murine mammary carcinoma cell line 4T1 and murine macrophage cell line RAW264.7 as an immune adjuvant, to obtain a biomimetic nanomedicine hybrid membrane@MnO_x@PpIX (HMMP) for vaccination and treatment of bacterial osteomyelitis. During the treatment, pathogen-associated antigens were released from the dead bacteria that aSDT killed, and the tumor cell membrane served as immunoadjuvant for recruiting and activating antigen presenting cells (APCs), such as dendritic cells and macrophages to promote antigen presentation. The synergic treatment of aSDT and immunotherapy by HMMP nanomedicine not only induced a potent antibacterial immune response and osteomyelitis regression, but also conferred the mice with long-lasting protective immunity against bacterial infection, as shown in Fig. 8.[167]

4.1.4 Other specific infectious diseases. *H. pylori* infection in the stomach affects more than 50% population all over the world, and is believed to be the leading inducement to gastric cancer, which is second leading cause of cancer mortality worldwide.[187] The global clinical guideline recommends triple therapy (proton pump inhibitor, clarithromycin, and amoxicillin or imidazole) as the first-line therapy for *H. pylori* infection. Still, it has been challenged by the development of AMR and adverse effects such as the undesired disruption of commensal bacteria.[188] Functional materials responsive to pH are potential candidates to address this issue. For example, the acidic environment in stomach could activate the antimicrobial property of HCT-AMPs by helix-to-coil transition and alleviate *H. pylori* burden by one hundred times compared with the control group *in vivo*. Moreover, it showed no toxicity to the commensal bacteria in the ileal contents and feces of mice because of the biocompatible helix conformation in physiological pH, while the triple therapy killed 65% and 86% of the commensal bacteria in the ileal contents and feces, respectively.[48]

Bacterial keratitis is an infection of cornea tissue that may lead to chronic corneal inflammation, perforation, and even blindness.[189] The leading cause of bacterial keratitis is the biofilm formed by the multidrug-resistant *P. aeruginosa* (MDR-*P. aeruginosa*),[190] which can hardly be treated with any of anti-pseudomonal antibiotics available in the clinic.[191] Hence, aPDT was used to combat the MDR-*P. aeruginosa*-associated

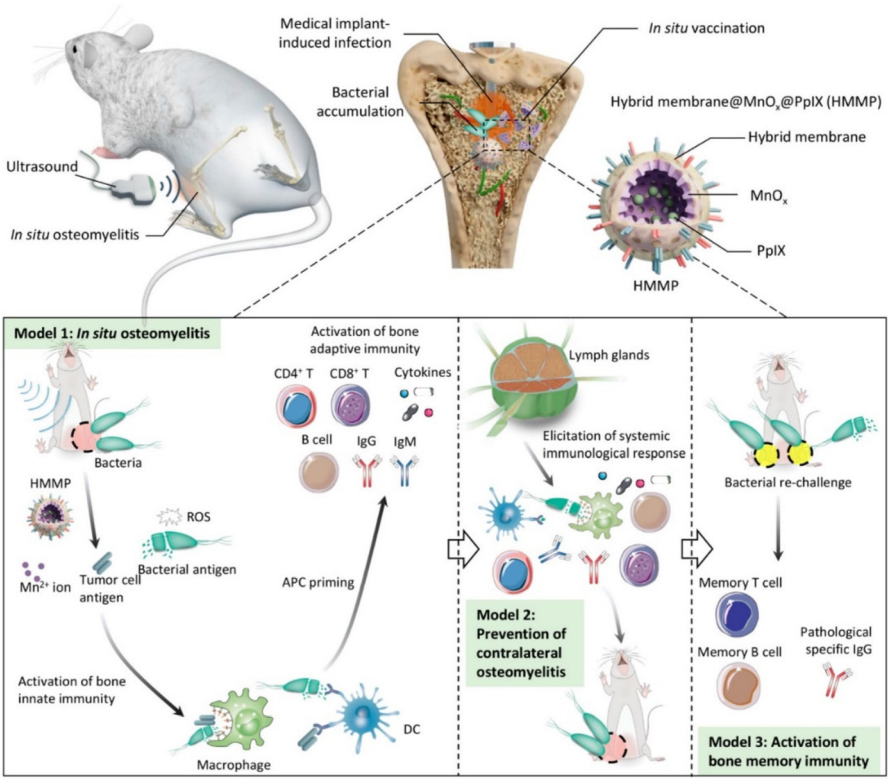

Fig. 8 Scheme of HMMP treatment and vaccination to bone infection. The dead bacterial antigens killed by ROS generated from HHMPs under ultrasound irradiation could activate bone adaptive immunity, which not only eliminated the infected pathogens but also conferred the body with long-lasting antibacterial immune memory. Reprinted with permission from ref. 167. Copyright 2022, American Chemical Society.

keratitis. As mentioned in the previous section, the nanoassembly consisting of the copolymer PαGal$_{50}$-*b*-PGRB$_n$ was developed, in which αGal had a targeting function, and RB was a PS (Fig. 9A).[132] After the copolymer-containing hydrogel was smeared on the cornea of the infected rabbit, it could specifically target MDR-*P. aeruginosa* by αGal-Lec A interaction, and the PS RB generated bactericidal ROS under light irradiation (578 nm, 0.06 W, 30 min). Compared with the untreated group, both the colony forming units (CFUs) and the concentration of an inflammatory factor interleukin-8 (IL-8) in the cornea of the treated group were significantly lower, indicating its excellent efficacy in killing the MDR-*P. aeruginosa* and relieve the infection-induced inflammation (Fig. 9B and C).

As the lung is exposed to a large quantity of air and potential pathogens, it has a high chance of being infected with bacteria. Note that most community-acquired pneumonias respond quickly to antibiotic treatment and infections can be cured without leaving residual marks on the lung. However, the patients with lung immunity or mucosal clearance disruption often suffer from the infection that difficult to be treated by conventional antibiotic.[192] The pulmonary infection is often accompanied by the overproduction of ROS, as an inflammatory response by immune cells to inhibit the growth of bacteria, but may also induce multidrug resistance.[193–196] This high-ROS microenvironment was taken advantage of for controlled release of moxifloxacin (MXF) to overcome its short clearance time. The borate ester-containing MXF/Oxi-αCD micelles responsively released its cargo by cleavage of ROS-liable borate ester in the presence of high concentration of H_2O_2. The DSPE-PEG-FA coating on the surface endowed them with the targeting property to macrophages at infection-induced inflammatory sites. Thus, the micelles exhibited greater *in vivo* antibacterial activity than free MXF against *P. aeruginosa*-infected lungs of immunodeficient mice due to their prolonged retention time at the lungs.[91] As urinary tract infection (UTI) aggravates oxidative stress in patients, the ROS-responsive selenocystamine linkages were introduced in the drug-conjugated nanoparticles to deliver ciprofloxacin, which is a well-established treatment for UTI but has side effects like diarrhea and opportunistic infections by disturbing the intestinal environment.[96]

4.2 Medical devices

4.2.1 Wound dressings. Skin, the largest organ of human body, plays a vital role in preventing the entry of external pathogens to protect the internal organs and tissues. In case of cutaneous injuries, the infection caused by pathogens would significantly impede the healing process, making the treatment painstaking and time-consuming. Thus, it requires elaborately designed wound care products.[197–199] The dressings carrying endogenous or exogenous stimuli-responsive antibacterial materials have been widely studied to prevent AMR and

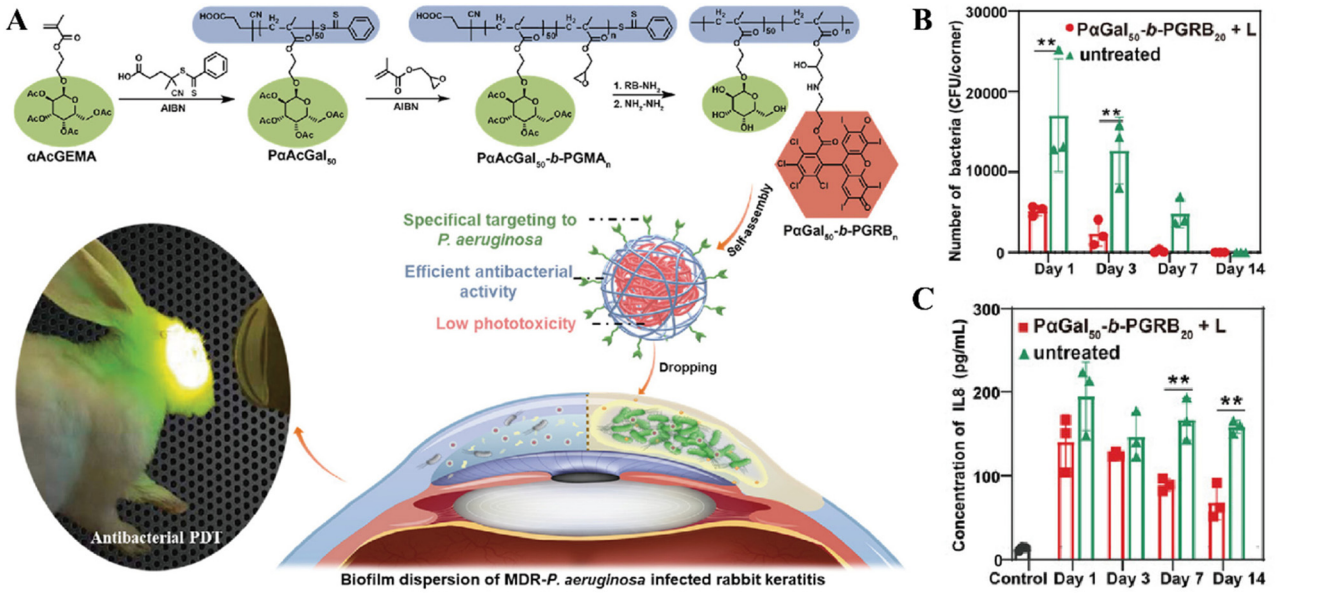

Fig. 9 (A) Schematic illustration of the bacteria-targeting nanoassembly for aPDT to treat MDR-*P. aeruginosa* biofilm-infected rabbit keratitis model. And the comparison of CFUs in MDR-*P. areuginosa* infected rabbit keratitis (B) and IL-8 in aqueous humor (C). Reprinted with permission from ref. 132. Copyright 2022, Wiley-VCH.

promote wound healing.[43,52,88–90,97,104,113,115,117,142,144,145,174,176] In this section, we mainly discuss the activatable antibacterial wound dressings for specific applications, including chronic, movable parts, post-operation, and burn wound healing.

Chronic wound is one of the common complications of diabetics, with over 15% morbidity among all diabetic patients. The high blood sugar level not only result in the narrowed blood vessels commonly so that fewer nutrients are carried to the injured area, but also lower the body's immune response so that the wounds are more susceptible to bacterial infection.[200] These factors make the wound healing process stagnate in the inflammation phase, while skin-repairing involves three sequential but overlapping processes: (1) acute inflammation, (2) angiogenesis/proliferation, and (3) remodeling.[201] Compared to normal tissues, the inflammatory sites are featured with a higher level of ROS and a lower pH. Hence, the variation in ROS and pH can be functioned as synergistic triggers to break the boronic ester bonds and Schiff base linkages integrated in the wound dressing materials and release the drugs smartly. Wang *et al.* reported a phenylboronic acid–diol ester bonds-crosslinked hydrogel (hydrogel@VAN-AgNCs&MIC, Fig. 10A), which carried an Ag nanoclusters (AgNCs)-vancomycin hybrid antibacterial system and a nonsteroidal anti-inflammatory drug nimesulide-encapsulated micelle (MIC). The hydrogel could be degraded in the infected wound, and then released the Van-AgNCs and nimesulide, as the boronic ester bonds could be cleaved by ROS and H^+. When the *S. aureus* infected wounds in the diabetic mice model were treated by the dressing of hydrogel@VAN-AgNCs&MIC, the wounds healed faster than the control groups with lower bacterial loads, as shown in Fig. 10B and C. Also, a strong suppression of the proinflammatory factors IL-6 and TNF-α were detected in the *in vitro* study, indicating a potent efficacy to alleviate the inflammation.[89]

Wound healing in movable parts such as joints and neck remains challenging because external mechanical forces can frequently disturb the healing process. As traditional wound dressings, such as gauzes and bandages, lack skin conformability, hydrogels with highly adjustable mechanical properties have been demonstrated a better candidate for healing of wounds in movable parts. For example, the mechano-responsive responsive hydrogel attached to the wound could frequently tolerate both tensile and compressive strains, triggering the release of the antibiotic-encapsulated micelles.[176] In another study, after applying the photosensitizer-loaded hydrogel to the *S. aureus* infected wound of the neck of mice, the hydrogel could well match the motions of the wound and fit closely with it. Upon NIR-irradiation, the wound closure process was accelerated, and no visible infection was observed.[115]

The infection by drug-resistant bacteria and tumor recurrence are the main obstructions to wound healing after skin tumor surgical treatment. PTT and PDT have exhibited excellent non-invasive efficacy against skin tumors and bacteria, thereby being used simultaneously against recurrent carcinoma and wound infection after the operation.[113,117] It should be noted that the release of PTA and chemotherapeutic agent can be controlled by both externally and internal stimuli. A recent research has demonstrated that indocyanine green (ICG) and doxorubicin (DOX) loaded in the cellulose nanofibers-based nanocage wound dressing (CNF-NWD) can be released upon the irradiation of NIR light and in an acidic

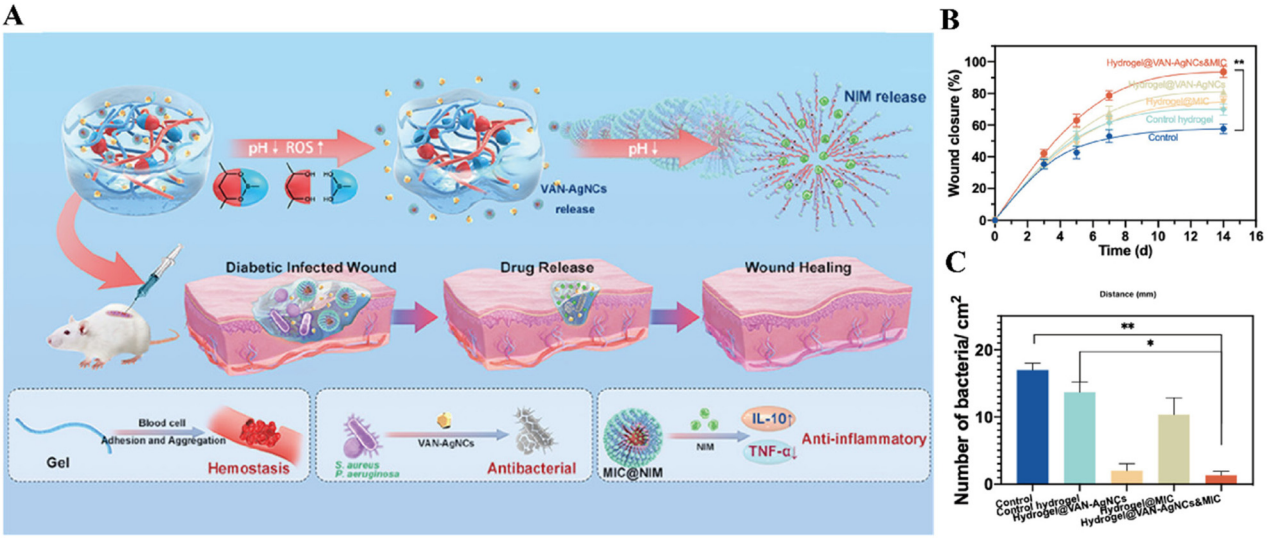

Fig. 10 (A) Schematic illustration of the pH and ROS dual-responsive hydrogel for diabetic infected wound dressing and its modes of action. (B) Quantitative results of wound closure. (C) Bacterial loads in different treatment groups on day 7. The hydrogel@VAN-AgNCs&MIC group showed a more complete wound healing and a lower bacterial load. Reprinted with permission from ref. 89. Copyright 2021, American Chemical Society.

microenvironment (pH 5.5–5.6) in the residual tumor cells after surgical resection, respectively.[117] Compared with control groups, the average volume of the melanoma on the BALB/c mice was significantly smaller as the tumor cells were killed by hyperthermia generated by ICG and the released DOX. And the MRSA-infected wound on the BALB/c mice recovered after the treatment because the localized heating promoted the elimination of pathogens, while the wound on control group still showed yellow pus on the 14th day of treatment, indicating a severe infection.

The wound caused by burn injuries are more vulnerable to infection than mechanical wounds, and their infections accounted for nearly 50% of burn injury deaths.[202] A pH-responsive wound dressing based on halloysite nanotube (HNT) composites was developed for controlled release of antibiotic minocycline. It achieved the ideal state for antibiotic delivery for burn wounds, in which a single dose for topical administration could afford an initial burst of drug for immediate tissue perfusion and a long-lasting and effective drug level at the wound site.[203] The burn wound created by the electric heater on mice healed almost entirely after 12 days of treatment with no infection detected, while no change in the wound size of the control group was observed and a high level of infection was recorded.[43]

4.2.2 Implant infections. The infection of biomedical implants has become one of the most frequent and severe diseases related to biomaterials, despite the fact that the development of implants has revolutionized modern medicine. Furthermore, biofilm formation and the immune escape of the adhered bacteria render corresponding antibiotic therapy harder than before.[204] For the on-demand treatment of the implant infection, the activatable antibacterial coatings were promising as they could be biocompatible at physiological status but bactericidal under the stimulation of infection-associated microenvironments or external signals. These materials have recently been studied against the infection of orthopedic, subcutaneous, and dental implants.

Artificial implants have been widely used as bone replacement nowadays, but they are also suffering from relatively high infection rate (*i.e.*, 0.7–4.2%) after orthopedic surgery, which could result in osteoarthritis or even amputation.[204,205] An ideal orthopedic implant should have both osteogenesis and antibacterial capability. To meet this requirement, black phosphorus nanosheets (BPs), a promising photothermal materials, were brought to the forefront as they can impart NIR-triggered aPTT and promot bone regeneration due to the naturally degraded PO_4^{3-}, as illustrated in Fig. 11A. The ZnL_2-BPs-integrated hydroxylapatite (HA) scaffold (ZnL_2-BPs@HAP) was implanted into the *S. aureus*-precontaminated bone defects of rats and was irradiated by NIR at a specific time point. The ZnL_2-BPs@HAP group had the lowest bacterial loads and the most excellent osteogenic ability confirmed by micro computed tomography (micro-CT) (Fig. 11B and C).[205] In another work, a cortical bone-mimicking polyetheretherketone (PEEK) was used as a support to carry copper and silver loaded silk fibroin (SF). The pH-responsive release of the metal ions was achieved by the change in electric charge and molecular conformation of SF with the shift in pH. Under physiological pH, a small amount of Cu^{2+} and Ag^{+} was released slowly from the implant to promote osteogenesis, while under an infection-induced acidic environment, a high concentration of metal ions was released for efficient bacterial killing.[206] Furthermore, thermo-responsive antibacterial surfaces are also suitable for bone implants by taking advantage of the difference between body and operation temperature. An anti-

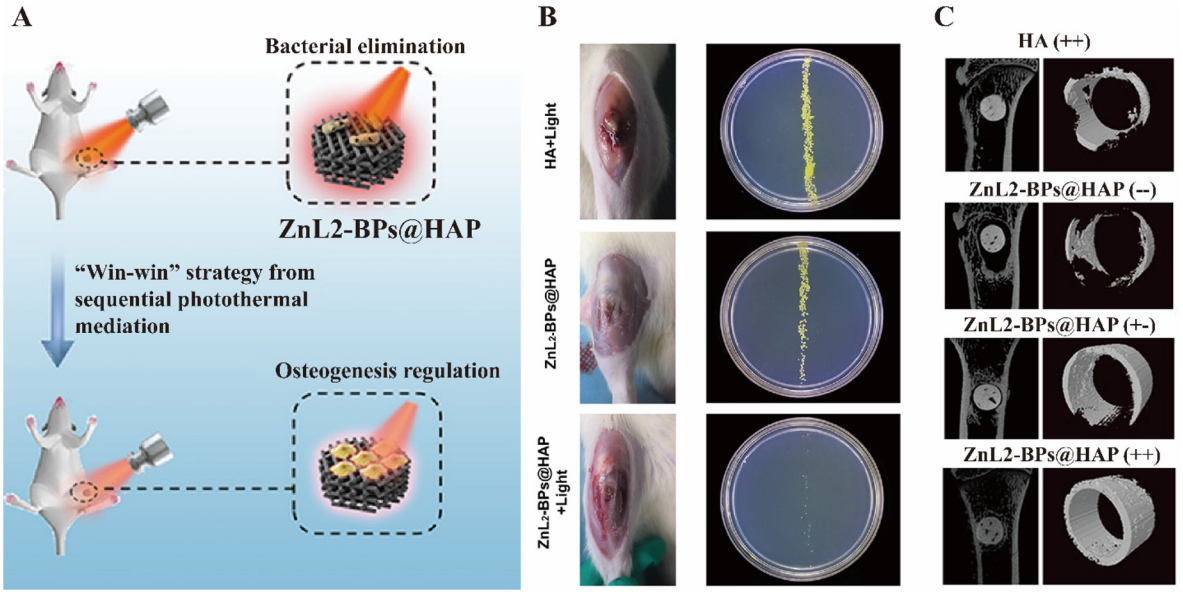

Fig. 11 (A) Schematic illustration of the dual-functional ZbL2-BPs@HAP to promote bacterial elimination and osteogenesis. (B) Photographs of the implant sites and bacterial colonies after two weeks post-implantation. (C) Micro-CT images of bone tissues surround the implants on the 10th week after surgery. The former+/– represents the presence/absence of irradiation I (NIR laser irradiation with 1.5 W cm^{-2} for 10 min each time on 1–3 days after surgery), and the latter+/– indicates the presence/absence of irradiation II (NIR laser irradiation with a smaller power of 1.0 W cm^{-2} for 6 min each time from the first week to sixth-week post-implantation). Reprinted with permission from ref. 205. Copyright 2021, American Chemical Society.

microbial peptide (AMP), HHC36, was conjugated to the thermo-responsive pNIPAM to build a smart surface.[207] At room temperature, the extended form of pNIPAM allowed the AMP to expose on the surface to kill any attached bacteria. Since this AMP is also cytotoxic to human tissue, when the surface was implanted in rabbit tibiae, the pNIPAM collapse to disguise the AMP inside to endow the surface with biocompatibility. This strategy guaranteed the implant being protected from bacterial infection before, during and after the orthopedic surgery to meet the clinical demands.

In addition to bone implantations, the subcutaneous implant infection models have also been widely used to test the efficacy of antimicrobial coatings on medical devices in preclinical studies.[35,63,105,208] In a recent report, two kinds of animal infection models were established to simulate both pre-operative and post-operative implant infection. In the first case, the implant material catheters, which were coated by the antibacterial PA and AG *via* pH-liable imine bonds as introduced in the previous section,[35] were soaked in *S. aureus* solution before subcutaneous implantation into the flank of mice. The other case was to inject *S. aureus* solution into the implanted regions directly. In both models, the bacterial colonies in the implanted devices as well as in several major organs were significantly lower in the coated implanted catheters group, indicating an excellent *in vivo* antibacterial activity of the pH-responsive coating materials. The subcutaneous infection can also be addressed with the kill-and-release strategy. A series of quaternary polyethylenimine (QPEI) was developed and coated on the surface of medical catheters for this purpose.[209] The side chain of QPEI can be degraded by acidic microenvironment or lipase to switch from biocidal cationic structure to bacteria-releasing zwitterionic forms. *In vivo* study demonstrated the smart coating effectively alleviate the bacterial burden on the implanted catheters and prevented the formation of biofilms.

The infection of a dental implant is the main reason for the failure of implant treatment, as the currently used abutments lack the ability to tightly anchor on soft tissue, while the interfacial integration between the abutment and the soft tissue can isolate the bacteria in the mouth. Yang *et al.* constructed a quasi-periodic titanium oxide metasurface on Ti alloy implants, which exhibited a photoactivated bacterial activity by generating ROS under NIR-irradiation. The Ti alloy combined with NIR light could alleviate *S. aureus* infection *in vivo*, promoting the proliferation of the human gingival fibroblasts and their expression of adhesion-related genes, which implies the beneficial biological effects of the Ti alloy implant.[25]

5. Conclusion and prospect

Stimuli-responsive antibacterial materials have shown great potential against infectious diseases and even antibiotic resistance. These materials are capable of precisely releasing their cargos at the infectious site, thereby achieving a higher localized concentration of antibiotics to kill pathogens and overcoming the off-target systemic adverse effects when free drugs are administrated. Notably, they can act in the ways that are

less likely to develop resistance by taking advantage of the ROS, hyperthermia, or sharpened edges produced in response to specific signals. This review emphasized on how the internal and external stimuli could activate these materials, and what the laboratorial therapeutic outcomes were. Many recent works have demonstrated the effectiveness of the stimuli-responsive antibacterial materials in both *in vitro* and *in vivo* studies.

Moreover, the host immune system plays vital roles against bacterial infection, and should be taken into consideration when developing the antibacterial materials. Some of the research introduced in this review reported the interaction of the fabricated materials with the immune system. They can function as immunogenic agents to boost the immune reactions,[167,168] when robust immune response is needed to eradicate the pathogens. On the other hand, in some infectious scenarios, the immune system is expected to be suppressed. For example, the wound healing requires a low inflammatory levels and host's foreign body response should be inhibited for a successful implantation. Thus, the anti-inflammatory property was considered when designing the responsive-antibacterial materials.[87,89,90,145] Additionally, some bacteria can exploit the immune cells to escape from the immune system itself, namely, they can survive and thrive in the immune cells after the uptake, which is known as intracellular infection.[210] Hence, antibacterial systems were designed to target and interact with the infected immune cells to eradicate the bacteria inside.[77,92] We believe the interaction and relationship of the biomaterials and the body immune system are of great importance, and more attention should be paid in this respect to fully understand the mode of actions of the stimuli-responsive antibacterial materials. Or else, the unclear interaction of the materials with the body could impede their clinical translation.

Though effective, most of these materials are still in the conceptual stage, and few examples of successful clinical translation have been reported. In the World Health Organization's (WHO) comprehensive report on the Antibacterial Agents in Clinical and Preclinical Development published in May 2022, it is summarized that the small-molecule antibiotics were still the largest category in both clinical study and preclinical pipeline.[211] Despite the non-traditional approaches constituted a relative great proportion of the total (34 out of 80 in clinical development phase, and 92 out of 217 in preclinical pipeline), the majority of which were bacteriophage-derived therapies and microbiome-modulating agents. Compared to traditional small-molecule antibiotics, the antibacterial mechanism of some responsive materials, such as metallic nanoparticles, have yet been thoroughly understood.[212] In addition, another problem faced by these non-conventional strategies was that they can hardly be applied to classical medicinal chemistry, which had been regulating the antibiotic studies.[213] Both reasons present major obstables that limit the clinical translations of this materials. On the other hand, the successful commercialization in the pharmaceutical industry requires not only the therapeutic efficacy of the drugs, but also the clinical safety and the feasibility of large-scale manufacturing.[11] A particular challenge for the responsive antibacterial materials is their potential safety concern, including direct cytotoxicity and nanoparticle accumulation-induced toxicity. As introduced in the previous section, the undesired release of drugs under physiological conditions may cause damages to healthy tissues, as many antibiotics themselves lack selectivity. In addition, some inorganic nanoparticles could induce toxicity by general mechanisms, such as nanoparticle-induced oxidative stress, size- and surface charge-depended toxicity, the perturbation of intracellular calcium, and the genotoxicity.[214] Once systemically administrated, the nano-scaled materials will be distributed in different organs, especially the liver, spleen, and kidney, according to their size, morphology, and other structural characteristics. Their long-term accumulation inside the body may have deleterious effects by possible mechanisms such as genetic toxicity, even though the concentration is non-cytotoxic *in vitro*.[215] Furthermore, the responsive mechanism of many systems introduced in this review is the release of biocidal payload upon stimulation. One concern with regards to this strategy is the leakage of drugs prior to the infection site, leading to non-specific systemic toxicity. Efforts to address the toxicity issue should be made. Another challenge to their clinical translation lies inlarge-scale manufacturing, as the laboratory preparation of these materials requires sophisticated synthesis. Therefore, it could be more attractive for industrial production if they have a simple structure with an explicit mode of action. The translational potential should be underscored in the future innovation of stimuli-responsive antibacterial materials, instead of decorating overly designed systems with complicated structures.

Finally, the *in vivo* studies introduced in this review for the treatment of specific diseases such as bone and oral infection cannot be established without the collaboration between chemists, materials scientists, biologists, and clinicians. The rational design by the scientists to ensure the effectiveness and the clinical input from the clinicians to clarify the practical needs are equally important for a successful medical product. We believe the extensive inter-disciplinary dialogue and cooperation will boost both the research and clinical translation and will be the future trend of developing responsive antibacterial materials.

Author contributions

BZ and HD conceived the concept of this review. BZ prepared the original draft and all authors contributed to the review and editing of the final manuscript.

Conflicts of interest

There are no conflicts to declare.

Acknowledgements

This work was supported by Ministry of Education-Singapore (MOE2018-T3-1-003 and MOE2018-T2-2-128).

References

1 J. Liu, O. Gefen, I. Ronin, M. Bar-Meir and N. Q. Balaban, *Science*, 2020, **367**, 200–204.
2 P. P. Kalelkar, M. Riddick and A. J. García, *Nat. Rev. Mater.*, 2022, **7**, 39–54.
3 C. J. Murray, K. S. Ikuta, F. Sharara, L. Swetschinski, G. R. Aguilar, A. Gray, C. Han, C. Bisignano, P. Rao and E. Wool, *Lancet*, 2022, **399**(10325), 629–655.
4 T. Thompson, *Nature*, 2022, DOI: **10.1038/d41586-022-00228-x**.
5 S. J. Dancer, *Lancet Infect. Dis.*, 2004, **4**, 611–619.
6 B. P. Willing, S. L. Russell and B. B. Finlay, *Nat. Rev. Microbiol.*, 2011, **9**, 233–243.
7 C. D. Fjell, J. A. Hiss, R. E. W. Hancock and G. Schneider, *Nat. Rev. Drug Discovery*, 2012, **11**, 37–51.
8 S. J. Lam, N. M. O'Brien-Simpson, N. Pantarat, A. Sulistio, E. H. H. Wong, Y.-Y. Chen, J. C. Lenzo, J. A. Holden, A. Blencowe, E. C. Reynolds and G. G. Qiao, *Nat. Microbiol.*, 2016, **1**, 16162.
9 J. M. Loeffler, D. Nelson and V. A. Fischetti, *Science*, 2001, **294**, 2170–2172.
10 D. Nelson, L. Loomis and V. A. Fischetti, *Proc. Natl. Acad. Sci. U. S. A.*, 2001, **98**, 4107–4112.
11 Y. Lu, A. A. Aimetti, R. Langer and Z. Gu, *Nat. Rev. Mater.*, 2016, **2**, 16075.
12 M. J. Mitchell, M. M. Billingsley, R. M. Haley, M. E. Wechsler, N. A. Peppas and R. Langer, *Nat. Rev. Drug Discovery*, 2021, **20**, 101–124.
13 M. A. C. Stuart, W. T. S. Huck, J. Genzer, M. Müller, C. Ober, M. Stamm, G. B. Sukhorukov, I. Szleifer, V. V. Tsukruk, M. Urban, F. Winnik, S. Zauscher, I. Luzinov and S. Minko, *Nat. Mater.*, 2010, **9**, 101–113.
14 X. Li, J. F. Lovell, J. Yoon and X. Chen, *Nat. Rev. Clin. Oncol.*, 2020, **17**, 657–674.
15 Y. Miyahara, N. Nagaya, M. Kataoka, B. Yanagawa, K. Tanaka, H. Hao, K. Ishino, H. Ishida, T. Shimizu, K. Kangawa, S. Sano, T. Okano, S. Kitamura and H. Mori, *Nat. Med.*, 2006, **12**, 459–465.
16 Y. Haraguchi, T. Shimizu, T. Sasagawa, H. Sekine, K. Sakaguchi, T. Kikuchi, W. Sekine, S. Sekiya, M. Yamato, M. Umezu and T. Okano, *Nat. Protoc.*, 2012, **7**, 850–858.
17 T. Wei, Y. Qu, Y. Zou, Y. Zhang and Q. Yu, *Curr. Opin. Chem. Eng.*, 2021, **34**, 100727.
18 R. S. Riley, C. H. June, R. Langer and M. J. Mitchell, *Nat. Rev. Drug Discovery*, 2019, **18**, 175–196.
19 J. Wang, Y. Li and G. Nie, *Nat. Rev. Mater.*, 2021, **6**, 766–783.
20 C. Tapeinos, H. Gao, T. Bauleth-Ramos and H. A. Santos, *Small*, 2022, 2200291.
21 A. S. Carlini, R. Gaetani, R. L. Braden, C. Luo, K. L. Christman and N. C. Gianneschi, *Nat. Commun.*, 2019, **10**, 1735.
22 S. Wang, Y. Gao, Q. Jin and J. Ji, *Biomater. Sci.*, 2020, **8**, 6825–6839.
23 D. Hu, H. Li, B. Wang, Z. Ye, W. Lei, F. Jia, Q. Jin, K.-F. Ren and J. Ji, *ACS Nano*, 2017, **11**, 9330–9339.
24 J. Zhang, Q. Jia, Z. Yue, J. Huo, J. Chai, L. Yu, R. Nie, H. Shao, Y. Zhao, P. Li and W. Huang, *Adv. Mater.*, 2022, **34**, 2200334.
25 M. Yang, S. Qiu, E. Coy, S. Li, K. Załęski, Y. Zhang, H. Pan and G. Wang, *Adv. Mater.*, 2022, **34**, 2106314.
26 G. Sachs, D. R. Scott and Y. Wen, *Curr. Gastroenterol. Rep.*, 2011, **13**, 540–546.
27 S. T. Reece and S. H. E. Kaufmann, in *Clinical Immunology*, ed. R. R. Rich, T. A. Fleisher, W. T. Shearer, H. W. Schroeder, A. J. Frew and C. M. Weyand, Elsevier, London, 4th edn, 2013, pp. 324–337.
28 K. Godha, K. M. Tucker, C. Biehl, D. F. Archer and S. Mirkin, *Gynecol. Endocrinol.*, 2018, **34**, 451–455.
29 H. Lambers, S. Piessens, A. Bloem, H. Pronk and P. Finkel, *Int. J. Cosmet. Sci.*, 2006, **28**, 359–370.
30 D. W. Landry and H. Bazari, in *Goldman's Cecil Medicine (Twenty Fourth Edition)*, ed. L. Goldman and A. I. Schafer and W. B. Saunders, Philadelphia, 2012, pp. 708–716.
31 K. B. Andersen and K. v. Meyenburg, *J. Bacteriol.*, 1980, **144**, 114–123.
32 S. M. Smith, *Antimicrob. Agents Chemother.*, 1991, **35**, 237–241.
33 S. Fuchs, J. Pané-Farré, C. Kohler, M. Hecker and S. Engelmann, *J. Bacteriol.*, 2007, **189**, 4275–4289.
34 S. C. Moldoveanu, in *Pyrolysis of Organic Molecules (Second Edition)*, ed. S. C. Moldoveanu, Elsevier, 2019, pp. 327–347.
35 L. Yang, C. Wang, L. Li, F. Zhu, X. Ren, Q. Huang, Y. Cheng and Y. Li, *Adv. Funct. Mater.*, 2022, **32**, 2108749.
36 J. Hu, Z. Zheng, C. Liu, Q. Hu, X. Cai, J. Xiao and Y. Cheng, *Biomater. Sci.*, 2019, **7**, 581–584.
37 P. Phoungtawee, F. Seidi, A. Treetong, C. Warin, A. Klamchuen and D. Crespy, *ACS Macro Lett.*, 2021, **10**, 365–369.
38 G. Zheng, J. Zheng, L. Xiao, T. Shang, Y. Cai, Y. Li, Y. Xu, X. Chen, Y. Liu and B. Yang, *ACS Omega*, 2021, **6**, 8672–8679.
39 J. Zhang, W. Zhu, B. Xin, S. Lin, L. Jin and H. Wang, *Biomater. Sci.*, 2019, **7**, 3795–3800.
40 R. S. Kalhapure, D. R. Sikwal, S. Rambharose, C. Mocktar, S. Singh, L. Bester, J. K. Oh, J. Renukuntla and T. Govender, *Nanomedicine*, 2017, **13**, 2067–2077.
41 X. Hao, W. Wang, Z. Yang, L. Yue, H. Sun, H. Wang, Z. Guo, F. Cheng and S. Chen, *Chem. Eng. J.*, 2019, **356**, 130–141.
42 Y. Liang, X. Zhao, P. X. Ma, B. Guo, Y. Du and X. Han, *J. Colloid Interface Sci.*, 2019, **536**, 224–234.
43 A. Mohebali and M. Abdouss, *Int. J. Biol. Macromol.*, 2020, **164**, 4193–4204.

44 X. Xie, T. Sun, J. Xue, Z. Miao, X. Yan, W. Fang, Q. Li, R. Tang, Y. Lu, L. Tang, Z. Zha and T. He, *Adv. Funct. Mater.*, 2020, **30**, 2000511.
45 W. Liang, J. Cheng, J. Zhang, Q. Xiong, M. Jin and J. Zhao, *ACS Nano*, 2022, **16**, 2762–2773.
46 Z. Chen, X. Lv, M. Zhao, P. Zhang, X. Ren and X. Mei, *Colloids Surf., B*, 2018, **170**, 648–655.
47 T. Yang, Y. Wu, X. Yue, C. Wang and J. Zhang, *J. Mater. Res.*, 2020, **35**, 2427–2440.
48 M. Xiong, Y. Bao, X. Xu, H. Wang, Z. Han, Z. Wang, Y. Liu, S. Huang, Z. Song, J. Chen, R. M. Peek, L. Yin, L.-F. Chen and J. Cheng, *Proc. Natl. Acad. Sci. U. S. A.*, 2017, **114**, 12675–12680.
49 P. Liu, G. Xu, D. Pranantyo, L. Q. Xu, K. G. Neoh and E. T. Kang, *ACS Biomater. Sci. Eng.*, 2018, **4**, 40–46.
50 J. Liang, F. Liu, J. Zou, H. H. K. Xu, Q. Han, Z. Wang, B. Li, B. Yang, B. Ren, M. Li, X. Peng, J. Li, S. Zhang, X. Zhou and L. Cheng, *J. Dent. Res.*, 2020, **99**, 1368–1376.
51 Y. Ohta, Y. Kondo, K. Kawada, T. Teranaka and N. Yoshino, *J. Oleo Sci.*, 2008, **57**, 445–452.
52 Y. Zu, Y. Wang, H. Yao, L. Yan, W. Yin and Z. Gu, *ACS Appl. Bio Mater.*, 2022, **5**(4), 1779–1793.
53 K. A. Natarajan, in *Biotechnology of Metals*, ed. K. A. Natarajan, Elsevier, Amsterdam, 2018, pp. 243–304.
54 L.-X. Yan, L.-J. Chen, X. Zhao and X.-P. Yan, *Adv. Funct. Mater.*, 2020, **30**, 1909042.
55 D. Hu, Y. Deng, F. Jia, Q. Jin and J. Ji, *ACS Nano*, 2020, **14**, 347–359.
56 B. Cezairliyan and F. M. Ausubel, *Proc. Natl. Acad. Sci. U. S. A.*, 2017, **114**, E7796–E7802.
57 B. Cadieux, V. Vijayakumaran, M. Bernards, M. McGavin and D. Heinrichs, *J. Bacteriol.*, 2014, **196**, 4044–4056.
58 M.-T. Nguyen, A. Luqman, K. Bitschar, T. Hertlein, J. Dick, K. Ohlsen, B. Bröker, B. Schittek and F. Götz, *Int. J. Med. Microbiol.*, 2018, **308**, 653–663.
59 *Rheumatology and Immunology Therapy*, ed. J. D. Abbott, G. Ball, D. Boumpas, S. L. Bridges, W. Chatham, J. Curtis, C. Daniel, L. B. Hughes, A. H. Kao, C. Langford, D. Lovell, S. Manzi, U. Müller-Ladner, H. C. Patel, R. A. S. Roubey, K. Saag, J. M. Sabatine, J. Shanahan, R. Simms, E. Smith, J. Sundy, A. J. Szalai, T. Wimmer and L. W. Moreland, Springer Berlin Heidelberg, Berlin, Heidelberg, 2004, pp. 411–412, DOI: 10.1007/3-540-29662-X_1273.
60 F. J. v. Natta, J. W. Hill and W. H. Carothers, *J. Am. Chem. Soc.*, 1934, **56**, 455–457.
61 Z. Gan, Q. Liang, J. Zhang and X. Jing, *Polym. Degrad. Stab.*, 1997, **56**, 209–213.
62 J. S. Chawla and M. M. Amiji, *Int. J. Pharm.*, 2002, **249**, 127–138.
63 A. Wang, S. Duan, X. Ding, N. Zhao, Y. Hu, X. Ding and F.-J. Xu, *Adv. Funct. Mater.*, 2021, **31**, 2011165.
64 J. Ma, S. Hou, D. Lu, B. Zhang, Q. Xiong, M. B. Chan-Park and H. Duan, *Macromol. Rapid Commun.*, 2022, **43**, 2100812.
65 J. Ma, S. Hou, M. B. Chan-Park and H. Duan, *Macromol. Rapid Commun.*, 2021, **42**, 2100255.
66 U. H. Ibrahim, N. Devnarain, C. A. Omolo, C. Mocktar and T. Govender, *Int. J. Pharm.*, 2021, **607**, 120960.
67 K. Rathnayake, U. Patel, C. Pham, A. McAlpin, T. Budisalich and S. N. Jayawardena, *ACS Appl. Bio Mater.*, 2020, **3**, 6708–6721.
68 H. Jung, *Arch. Plast. Surg.*, 2020, **47**, 297–300.
69 P. Ayaz, B. Xu, X. Zhang, J. Wang, D. Yu and J. Wu, *Appl. Surf. Sci.*, 2020, **527**, 146806.
70 P. Liu, Y. Hao, Y. Ding, Z. Yuan, Y. Liu and K. Cai, *J. Mater. Sci.: Mater. Med.*, 2018, **29**, 160.
71 Z. Yuan, S. Huang, S. Lan, H. Xiong, B. Tao, Y. Ding, Y. Liu, P. Liu and K. Cai, *J. Mater. Chem. B*, 2018, **6**, 8090–8104.
72 Y. Yu, Q. Ran, X. Shen, H. Zheng and K. Cai, *Colloids Surf., B*, 2020, **185**, 110592.
73 X. Wang, J. Wu, P. Li, L. Wang, J. Zhou, G. Zhang, X. Li, B. Hu and X. Xing, *ACS Appl. Mater. Interfaces*, 2018, **10**, 34905–34915.
74 Y. Liu, A. Lin, J. Liu, X. Chen, X. Zhu, Y. Gong, G. Yuan, L. Chen and J. Liu, *ACS Appl. Mater. Interfaces*, 2019, **11**, 26590–26606.
75 J. L. Millán, *Purinergic Signalling*, 2006, **2**, 335–341.
76 N. Li, L. Jiang, H. Jin, Y. Wu, Y. Liu, W. Huang, L. Wei, Q. Zhou, F. Chen, Y. Gao, B. Zhu and X. Zhang, *Colloids Surf., B*, 2019, **183**, 110454.
77 M. Chen, J. He, S. Xie, T. Wang, P. Ran, Z. Zhang and X. Li, *J. Controlled Release*, 2020, **322**, 326–336.
78 P. Dasari, M. Nordengrün, C. Vilhena, L. Steil, G. Abdurrahman, K. Surmann, V. Dhople, J. Lahrberg, C. Bachert, C. Skerka, U. Völker, B. M. Bröker and P. F. Zipfel, *J. Bacteriol.*, 2022, **204**, e0018421.
79 Y. Zhang, K. Hu, X. Xing, J. Zhang, M.-R. Zhang, X. Ma, R. Shi and L. Zhang, *Macromol. Biosci.*, 2021, **21**, 2000194.
80 Y.-M. Zuo, X. Yan, J. Xue, L.-Y. Guo, W.-W. Fang, T.-C. Sun, M. Li, Z. Zha, Q. Yu, Y. Wang, M. Zhang, Y. Lu, B. Cao and T. He, *ACS Appl. Mater. Interfaces*, 2020, **12**, 4333–4342.
81 Y. Ding, Y. Hao, Z. Yuan, B. Tao, M. Chen, C. Lin, P. Liu and K. Cai, *Biomater. Sci.*, 2020, **8**, 1840–1854.
82 L. Qiu, C. Wang, X. Lei, X. Du, Q. Guo, S. Zhou, P. Cui, T. Hong, P. Jiang, J. Wang, Y.-Q. Li and J. Xia, *Biomater. Sci.*, 2021, **9**, 3433–3444.
83 T. M. Koyasseril-Yehiya, A. García-Heredia, F. Anson, P. Rangadurai, M. S. Siegrist and S. Thayumanavan, *Nanoscale*, 2020, **12**, 20693–20698.
84 C. N. Paiva and M. T. Bozza, *Antioxid. Redox Signal.*, 2014, **20**, 1000–1037.
85 A. Stubelius, S. Lee and A. Almutairi, *Acc. Chem. Res.*, 2019, **52**, 3108–3119.
86 Y. Zhang, P. Feng, J. Yu, J. Yang, J. Zhao, J. Wang, Q. Shen and Z. Gu, *Adv. Ther.*, 2018, **1**, 1800035.
87 C. Hu, F. Zhang, L. Long, Q. Kong, R. Luo and Y. Wang, *J. Controlled Release*, 2020, **324**, 204–217.
88 W. Shi, Y. Kong, Y. Su, M. A. Kuss, X. Jiang, X. Li, J. Xie and B. Duan, *J. Mater. Chem. B*, 2021, **9**, 7182–7195.
89 Y. Wang, Y. Wu, L. Long, L. Yang, D. Fu, C. Hu, Q. Kong and Y. Wang, *ACS Appl. Mater. Interfaces*, 2021, **13**, 33584–33599.

90 Y. Wu, Y. Wang, L. Long, C. Hu, Q. Kong and Y. Wang, *J. Controlled Release*, 2022, **341**, 147–165.
91 Y. Wang, Q. Yuan, W. Feng, W. Pu, J. Ding, H. Zhang, X. Li, B. Yang, Q. Dai, L. Cheng, J. Wang, F. Sun and D. Zhang, *J. Nanobiotechnol.*, 2019, **17**, 103.
92 J. Qiao, S. Cui and M. P. Xiong, *J. Mater. Chem. B*, 2021, **9**, 8951–8961.
93 A. Rinaldi, R. Caraffi, M. V. Grazioli, N. Oddone, L. Giardino, G. Tosi, M. A. Vandelli, L. Calzà, B. Ruozi and J. T. Duskey, *Polymers*, 2022, **14**, 687.
94 J. Li, Z. Ding, Y. Li, J. Miao, W. Wang, K. Nundlall and S. Chen, *Mater. Des.*, 2020, **195**, 109021.
95 V. G. Deepagan, S. Kwon, D. G. You, V. Q. Nguyen, W. Um, H. Ko, H. Lee, D.-G. Jo, Y. M. Kang and J. H. Park, *Biomaterials*, 2016, **103**, 56–66.
96 J. Song, M.-S. Kook, B.-H. Kim, Y.-I. Jeong and K.-J. Oh, *Materials*, 2021, **14**, 4125.
97 X. Han, R. Yang, X. Wan, J. Dou, J. Yuan, B. Chi and J. Shen, *J. Mater. Chem. B*, 2021, **9**, 6212–6225.
98 D. Morris, M. Khurasany, T. Nguyen, J. Kim, F. Guilford, R. Mehta, D. Gray, B. Saviola and V. Venketaraman, *Biochim. Biophys. Acta, Gen. Subj.*, 2013, **1830**, 3329–3349.
99 M. M. Lu, Y. Ge, J. Qiu, D. Shao, Y. Zhang, J. Bai, X. Zheng, Z. M. Chang, Z. Wang, W. F. Dong and C. B. Tang, *Int. J. Nanomed.*, 2018, **13**, 7697–7709.
100 Y. Zhang, Y. Pi, Y. Hua, J. Xie, C. Wang, K. Guo, Z. Zhao and Y. Yong, *Theranostics*, 2020, **10**, 10031–10045.
101 Y. Fu, Y. Wang, L. Huang, S. Xiao, F. Chen, P. Fan, M. Zhong, J. Tan and J. Yang, *Ind. Eng. Chem. Res.*, 2018, **57**, 8938–8945.
102 L. Huang, L. Zhang, S. Xiao, Y. Yang, F. Chen, P. Fan, Z. Zhao, M. Zhong and J. Yang, *Chem. Eng. J.*, 2018, **333**, 1–10.
103 Y. Wang, J. Wu, D. Zhang, F. Chen, P. Fan, M. Zhong, S. Xiao, Y. Chang, X. Gong, J. Yang and J. Zheng, *J. Mater. Chem. B*, 2019, **7**, 5762–5774.
104 J. Yuan, D. Zhang, X. He, Y. Ni, L. Che, J. Wu, B. Wu, Y. Wang, S. Wang, D. Sha, S. Y. Zheng and J. Yang, *Int. J. Biol. Macromol.*, 2021, **190**, 754–762.
105 Z. Liu, Y. Yi, L. Song, Y. Chen, L. Tian, J. Zhao and L. Ren, *Acta Biomater.*, 2022, **141**, 198–208.
106 Y. Wu, Z. Song, H. Wang and H. Han, *Nat. Commun.*, 2019, **10**, 4464.
107 Y. Huang, L. Zou, J. Wang, Q. Jin and J. Ji, *WIREs Nanomed. Nanobiotechnol.*, 2022, e1775.
108 A. Cavallaro, S. Taheri and K. Vasilev, *Biointerphases*, 2014, **9**, 029005.
109 X. Wang, M. Shan, S. Zhang, X. Chen, W. Liu, J. Chen and X. Liu, *Adv. Sci.*, 2022, **9**, 2104843.
110 Y. Ren, H. Liu, X. Liu, Y. Zheng, Z. Li, C. Li, K. W. K. Yeung, S. Zhu, Y. Liang, Z. Cui and S. Wu, *Cell Rep. Phys. Sci.*, 2020, **1**, 100245.
111 X. Jiang, X. Fan, W. Xu, R. Zhang and G. Wu, *ACS Biomater. Sci. Eng.*, 2019, **6**, 680–689.
112 S. Wu, A. Li, X. Zhao, C. Zhang, B. Yu, N. Zhao and F.-J. Xu, *ACS Appl. Mater. Interfaces*, 2019, **11**, 17177–17183.
113 W. Niu, M. Chen, Y. Guo, M. Wang, M. Luo, W. Cheng, Y. Wang and B. Lei, *ACS Nano*, 2021, **15**, 14323–14337.
114 N. Yang, H. Guo, C. Cao, X. Wang, X. Song, W. Wang, D. Yang, L. Xi, X. Mou and X. Dong, *Biomaterials*, 2021, **275**, 120918.
115 Y. Li, P. Yu, J. Wen, H. Sun, D. Wang, J. Liu, J. Li and H. Chu, *Adv. Funct. Mater.*, 2022, **32**, 2110720.
116 S. Tian, H. Bai, S. Li, Y. Xiao, X. Cui, X. Li, J. Tan, Z. Huang, D. Shen, W. Liu, P. Wang, B. Z. Tang and C.-S. Lee, *Angew. Chem., Int. Ed.*, 2021, **60**, 11758–11762.
117 R. Chen, C. Zhao, Z. Chen, X. Shi, H. Zhu, Q. Bu, L. Wang, C. Wang and H. He, *Biomaterials*, 2022, **281**, 121330.
118 M. Ding and D. Chen, in *Nanoarchitectonics for Smart Delivery and Drug Targeting*, ed. A. M. Holban and A. M. Grumezescu, William Andrew Publishing, 2016, pp. 227–260.
119 J. Shi, J. Li, Y. Wang, J. Cheng and C. Y. Zhang, *J. Mater. Chem. B*, 2020, **8**, 5793–5807.
120 J. Li, W. Zhang, W. Ji, J. Wang, N. Wang, W. Wu, Q. Wu, X. Hou, W. Hu and L. Li, *J. Mater. Chem. B*, 2021, **9**, 7909–7926.
121 J. Huo, Q. Jia, H. Huang, J. Zhang, P. Li, X. Dong and W. Huang, *Chem. Soc. Rev.*, 2021, **50**, 8762–8789.
122 L. Sun, Y. Wang, F. Yang, X. Zhang and W. Hu, *Adv. Mater.*, 2019, **31**, 1902328.
123 M. Klessinger and J. Michl, *Excited states and photochemistry of organic molecules*, VCH publishers, 1995.
124 L. Sun, W. Zhu, W. Wang, F. Yang, C. Zhang, S. Wang, X. Zhang, R. Li, H. Dong and W. Hu, *Angew. Chem., Int. Ed.*, 2017, **56**, 7831–7835.
125 C. S. Foote, *Journal*, 1991, **54**, 659–659.
126 C. Liao, Y. Li and S. C. Tjong, *Nanomaterials*, 2020, **10**, 124.
127 L. Marín-Caba, G. Bodelón, Y. Negrín-Montecelo and M. A. Correa-Duarte, *Adv. Funct. Mater.*, 2021, **31**, 2105807.
128 A. Sousa-Castillo, M. Comesaña-Hermo, B. Rodríguez-González, M. Pérez-Lorenzo, Z. Wang, X.-T. Kong, A. O. Govorov and M. A. Correa-Duarte, *J. Phys. Chem. C*, 2016, **120**, 11690–11699.
129 C. Feng, D. Zhu, L. Chen, Y. Lu, J. Liu, N. Y. Kim, S. Liang, X. Zhang, Y. Lin, Y. Ma and C. Dong, *Front. Pharmacol.*, 2019, **10**, 369.
130 X. Tang, X. Chen, S. Zhang, X. Gu, R. Wu, T. Huang, Z. Zhou, C. Sun, J. Ling, M. Liu and Y. Yang, *Adv. Funct. Mater.*, 2021, **31**, 2101320.
131 R. López-Igual, J. Bernal-Bayard, A. Rodríguez-Patón, J.-M. Ghigo and D. Mazel, *Nat. Biotechnol.*, 2019, **37**, 755–760.
132 Y. Zhu, S. Wu, Y. Sun, X. Zou, L. Zheng, S. Duan, J. Wang, B. Yu, R. Sui and F.-J. Xu, *Adv. Funct. Mater.*, 2022, **32**, 2111066.
133 Q. Bai, M. Liang, W. Wu, C. Zhang, X. Li, M. Liu, D. Yang, W. W. Yu, Q. Hu, L. Wang, F. Du, N. Sui and Z. Zhu, *Adv. Funct. Mater.*, 2022, **32**, 2112683.
134 X. Hou, H. Zeng, X. Chi and X. Hu, *Nano Lett.*, 2021, **21**, 9966–9975.

135 G. Zhang, Y. Yang, J. Shi, X. Yao, W. Chen, X. Wei, X. Zhang and P. K. Chu, *Biomaterials*, 2021, **269**, 120634.
136 X. Zhou, Z. Wang, Y. K. Chan, Y. Yang, Z. Jiao, L. Li, J. Li, K. Liang and Y. Deng, *Adv. Funct. Mater.*, 2022, **32**, 2109469.
137 S. Hou, S. H. Mahadevegowda, V. C. Mai, M. B. Chan-Park and H. Duan, *Adv. Ther.*, 2019, **2**, 1900052.
138 T. Wei, W. Zhan, Q. Yu and H. Chen, *ACS Appl. Mater. Interfaces*, 2017, **9**, 25767–25774.
139 Q. Liu and L. Liu, *Langmuir*, 2019, **35**, 1450–1457.
140 K. N. Plunkett, X. Zhu, J. S. Moore and D. E. Leckband, *Langmuir*, 2006, **22**, 4259–4266.
141 G. Graziano, *Int. J. Biol. Macromol.*, 2000, **27**, 89–97.
142 C. Chen, Y. Liu, L. Sun, G. Chen, X. Wu, J. Ren and Y. Zhao, *ACS Appl. Bio Mater.*, 2019, **2**, 2155–2161.
143 W. Kang, J. Liang, T. Liu, H. Long, L. Huang, Q. Shi, J. Zhang, S. Deng and S. Tan, *Int. J. Biol. Macromol.*, 2022, **200**, 99–109.
144 J. S. Paneysar, S. Barton, P. Ambre and E. Coutinho, *J. Pharm. Sci.*, 2022, **111**, 810–817.
145 W.-C. Huang, R. Ying, W. Wang, Y. Guo, Y. He, X. Mo, C. Xue and X. Mao, *Adv. Funct. Mater.*, 2020, **30**, 2000644.
146 G. Qing, X. Zhao, N. Gong, J. Chen, X. Li, Y. Gan, Y. Wang, Z. Zhang, Y. Zhang, W. Guo, Y. Luo and X.-J. Liang, *Nat. Commun.*, 2019, **10**, 4336.
147 H. Zhang, Z. Zhang, H. Zhang, C. Chen, D. Zhang and Y. Zhao, *ACS Appl. Mater. Interfaces*, 2021, **13**, 18413–18422.
148 T. Wei, Z. Tang, Q. Yu and H. Chen, *ACS Appl. Mater. Interfaces*, 2017, **9**, 37511–37523.
149 X. Wang, S. Yan, L. Song, H. Shi, H. Yang, S. Luan, Y. Huang, J. Yin, A. F. Khan and J. Zhao, *ACS Appl. Mater. Interfaces*, 2017, **9**, 40930–40939.
150 Y. Ni, D. Zhang, Y. Wang, X. He, J. He, H. Wu, J. Yuan, D. Sha, L. Che, J. Tan and J. Yang, *ACS Appl. Mater. Interfaces*, 2021, **13**, 14543–14551.
151 Y. Wang, T. Wei, Y. Qu, Y. Zhou, Y. Zheng, C. Huang, Y. Zhang, Q. Yu and H. Chen, *ACS Appl. Mater. Interfaces*, 2020, **12**, 21283–21291.
152 L. Xie, X. Pang, X. Yan, Q. Dai, H. Lin, J. Ye, Y. Cheng, Q. Zhao, X. Ma, X. Zhang, G. Liu and X. Chen, *ACS Nano*, 2020, **14**, 2880–2893.
153 A. A. Balhaddad, Y. Xia, Y. Lan, L. Mokeem, M. S. Ibrahim, M. D. Weir, H. H. K. Xu and M. A. S. Melo, *ACS Nano*, 2021, **15**, 19888–19904.
154 X. Lu, X. Feng, J. R. Werber, C. Chu, I. Zucker, J.-H. Kim, C. O. Osuji and M. Elimelech, *Proc. Natl. Acad. Sci. U. S. A.*, 2017, **114**, E9793–E9801.
155 K. Zheng, K. Li, T.-H. Chang, J. Xie and P.-Y. Chen, *Adv. Funct. Mater.*, 2019, **29**, 1904603.
156 A. Elbourne, S. Cheeseman, P. Atkin, N. P. Truong, N. Syed, A. Zavabeti, M. Mohiuddin, D. Esrafilzadeh, D. Cozzolino, C. F. McConville, M. D. Dickey, R. J. Crawford, K. Kalantar-Zadeh, J. Chapman, T. Daeneke and V. K. Truong, *ACS Nano*, 2020, **14**, 802–817.
157 S. Dutz and R. Hergt, *Int. J. Hyperthermia*, 2013, **29**, 790–800.
158 Q. Ding, D. Liu, D. Guo, F. Yang, X. Pang, R. Che, N. Zhou, J. Xie, J. Sun, Z. Huang and N. Gu, *Biomaterials*, 2017, **124**, 35–46.
159 M. S. Alavijeh, M. S. Bani, I. Rad, S. Hatamie, M. S. Zomorod and M. Haghpanahi, *J. Mech. Sci. Technol.*, 2021, **35**, 815–821.
160 S. Hou, S. H. Mahadevegowda, D. Lu, K. Zhang, M. B. Chan-Park and H. Duan, *Small*, 2021, **17**, 2006357.
161 W. Chen, C. A. Glackin, M. A. Horwitz and J. I. Zink, *Acc. Chem. Res.*, 2019, **52**, 1531–1542.
162 Q. Yu, T. Deng, F.-C. Lin, B. Zhang and J. I. Zink, *ACS Nano*, 2020, **14**, 5926–5937.
163 X. Wang, X. Zhong, F. Gong, Y. Chao and L. Cheng, *Mater. Horiz.*, 2020, **7**, 2028–2046.
164 J. Roy, V. Pandey, I. Gupta and H. Shekhar, *ACS Biomater. Sci. Eng.*, 2021, **7**, 5326–5338.
165 D. Costley, C. Mc Ewan, C. Fowley, A. P. McHale, J. Atchison, N. Nomikou and J. F. Callan, *Int. J. Hyperthermia*, 2015, **31**, 107–117.
166 Y. Yu, L. Tan, Z. Li, X. Liu, Y. Zheng, X. Feng, Y. Liang, Z. Cui, S. Zhu and S. Wu, *ACS Nano*, 2021, **15**, 10628–10639.
167 H. Lin, C. Yang, Y. Luo, M. Ge, H. Shen, X. Zhang and J. Shi, *ACS Nano*, 2022, **16**, 5943–5960.
168 X. Pang, X. Liu, Y. Cheng, C. Zhang, E. Ren, C. Liu, Y. Zhang, J. Zhu, X. Chen and G. Liu, *Adv. Mater.*, 2019, **31**, 1902530.
169 X. Feng, J. Lei, L. Ma, Q. Ouyang, Y. Zeng, H. Liang, C. Lei, G. Li, L. Tan, X. Liu and C. Yang, *Small*, 2022, **18**, 2105775.
170 H. Liu, J. Li, X. Liu, Z. Li, Y. Zhang, Y. Liang, Y. Zheng, S. Zhu, Z. Cui and S. Wu, *ACS Nano*, 2021, **15**, 18505–18519.
171 E. Cantini, X. Wang, P. Koelsch, J. A. Preece, J. Ma and P. M. Mendes, *Acc. Chem. Res.*, 2016, **49**, 1223–1231.
172 X. Wang, M. Shan, S. Zhang, X. Chen, W. Liu, J. Chen and X. Liu, *Adv. Sci.*, 2022, **9**, 2104843.
173 S. Liu, H. Yuan, H. Bai, P. Zhang, F. Lv, L. Liu, Z. Dai, J. Bao and S. Wang, *J. Am. Chem. Soc.*, 2018, **140**, 2284–2291.
174 X. Zhao, L.-Y. Wang, C.-Y. Tang, X.-J. Zha, Y. Liu, B.-H. Su, K. Ke, R.-Y. Bao, M.-B. Yang and W. Yang, *ACS Nano*, 2020, **14**, 8793–8805.
175 P. Das, C. K. Yeo, J. Ma, K. Phan, P. Chen, M. B. Chan-Park and H. Duan, *ACS Appl. Nano Mater.*, 2018, **1**, 940–952.
176 K. Fang, R. Wang, H. Zhang, L. Zhou, T. Xu, Y. Xiao, Y. Zhou, G. Gao, J. Chen, D. Liu, F. Ai and J. Fu, *ACS Appl. Mater. Interfaces*, 2020, **12**, 52307–52318.
177 N. V. Ayala-núñez, H. H. Lara Villegas, L. del Carmen Ixtepan Turrent and C. Rodríguez Padilla, *Nanobiotechnology*, 2009, **5**, 2–9.
178 A. J. Huh and Y. J. Kwon, *J. Controlled Release*, 2011, **156**, 128–145.

179 N. Osman, C. A. Omolo, R. Gannimani, A. Y. Waddad, S. Rambharose, C. Mocktar, S. Singh, R. Parboosing and T. Govender, *J. Drug Delivery Sci. Technol.*, 2019, **53**, 101125.
180 L. Poirel, J.-Y. Madec, A. Lupo, A.-K. Schink, N. Kieffer, P. Nordmann and S. Schwarz, *Microbiol. Spectrum*, 2018, **6**(4), 6.4.14.
181 M. Bassetti, E. Righi, A. Carnelutti, E. Graziano and A. Russo, *Expert Rev. Anti-Infect. Ther.*, 2018, **16**, 749–761.
182 I. W. Sutherland, *Trends Microbiol.*, 2001, **9**, 222–227.
183 T. Kanno, K. Nakamura, K. Ishiyama, Y. Yamada, M. Shirato, Y. Niwano, C. Kayaba, K. Ikeda, A. Takagi and T. Yamaguchi, *Sci. Rep.*, 2017, **7**, 1–10.
184 Z. Nazar Majeed, K. Philip, A. Alabsi, S. Pushparajan and D. Swaminathan, *Dis. Markers*, 2016, **2016**, 1804727.
185 Y. Jiao, F. R. Tay, L.-n. Niu and J.-h. Chen, *Int. J. Oral Sci.*, 2019, **11**, 1–11.
186 M. I. Hofstee, G. Muthukrishnan, G. J. Atkins, M. Riool, K. Thompson, M. Morgenstern, M. J. Stoddart, R. G. Richards, S. A. J. Zaat and T. F. Moriarty, *Am. J. Pathol.*, 2020, **190**, 1151–1163.
187 N. Kodaman, A. Pazos, B. G. Schneider, M. B. Piazuelo, R. Mera, R. S. Sobota, L. A. Sicinschi, C. L. Shaffer, J. Romero-Gallo, T. de Sablet, R. H. Harder, L. E. Bravo, R. M. Peek, K. T. Wilson, T. L. Cover, S. M. Williams and P. Correa, *Proc. Natl. Acad. Sci. U. S. A.*, 2014, **111**, 1455–1460.
188 P. Malfertheiner, *Nat. Rev. Gastroenterol. Hepatol.*, 2010, **7**, 538–539.
189 D. S. J. Ting, C. S. Ho, R. Deshmukh, D. G. Said and H. S. Dua, *Eye*, 2021, **35**, 1084–1101.
190 A. Thanabalasuriar, B. N. V. Scott, M. Peiseler, M. E. Willson, Z. Zeng, P. Warrener, A. E. Keller, B. G. J. Surewaard, E. A. Dozier, J. T. Korhonen, L.I. Cheng, M. Gadjeva, C. K. Stover and A. DiGiandomenico, *Cell Host Microbe*, 2019, **25**(4), 526–536.
191 S. Wagner, R. Sommer, S. Hinsberger, C. Lu, R. W. Hartmann, M. Empting and A. Titz, *J. Med. Chem.*, 2016, **59**, 5929–5969.
192 A. A. Pragman, J. P. Berger and B. J. Williams, *Clin. Pulm. Med.*, 2016, **23**, 57–66.
193 D. P. Rosanna and C. Salvatore, *Curr. Pharm. Des.*, 2012, **18**, 3889–3900.
194 S. Selemidis, *Respirology*, 2019, **24**, 15–16.
195 H. H. Ware, V. V. Kulkarni, Y. Wang, J. Pantaleón García, M. Leiva Juarez, C. T. Kirkpatrick, S. Wali, S. Syed, A. D. Kontoyiannis, W. K. A. Sikkema, J. M. Tour and S. E. Evans, *PLoS One*, 2019, **14**, e0208216.
196 J. A. Imlay, *Annu. Rev. Microbiol.*, 2015, **69**, 93–108.
197 Y. Belkaid and J. A. Segre, *Science*, 2014, **346**, 954–959.
198 H. S. Kim, X. Sun, J.-H. Lee, H.-W. Kim, X. Fu and K. W. Leong, *Adv. Drug Delivery Rev.*, 2019, **146**, 209–239.
199 M. M. Mihai, M. B. Dima, B. Dima and A. M. Holban, *Materials*, 2019, **12**, 2176.
200 W. J. Jeffcoate and K. G. Harding, *Lancet*, 2003, **361**, 1545–1551.
201 J. Yan, G. Tie, S. Wang, A. Tutto, N. DeMarco, L. Khair, T. G. Fazzio and L. M. Messina, *Nat. Commun.*, 2018, **9**, 1–13.
202 F. N. Williams, D. N. Herndon, H. K. Hawkins, J. O. Lee, R. A. Cox, G. A. Kulp, C. C. Finnerty, D. L. Chinkes and M. G. Jeschke, *Crit. Care*, 2009, **13**, 1–7.
203 J. A. Setterstrom, T. R. Tice and W. E. Myers, in *Recent advances in drug delivery systems*, Springer, 1984, pp. 185–198.
204 C. R. Arciola, D. Campoccia and L. Montanaro, *Nat. Rev. Microbiol.*, 2018, **16**, 397–409.
205 Y. Wu, Q. Liao, L. Wu, Y. Luo, W. Zhang, M. Guan, H. Pan, L. Tong, P. K. Chu and H. Wang, *ACS Nano*, 2021, **15**, 17854–17869.
206 J. Yan, D. Xia, W. Zhou, Y. Li, P. Xiong, Q. Li, P. Wang, M. Li, Y. Zheng and Y. Cheng, *Acta Biomater.*, 2020, **115**, 220–234.
207 J. Zhan, L. Wang, Y. Zhu, H. Gao, Y. Chen, J. Chen, Y. Jia, J. He, Z. Fang, Y. Zhu, C. Mao, L. Ren and Y. Wang, *ACS Appl. Mater. Interfaces*, 2018, **10**, 35830–35837.
208 B. Wang, H. Liu, Z. Wang, S. Shi, K. Nan, Q. Xu, Z. Ye and H. Chen, *J. Mater. Chem. B*, 2017, **5**, 1498–1506.
209 J. Hoque, S. Ghosh, K. Paramanandham and J. Haldar, *ACS Appl. Mater. Interfaces*, 2019, **11**, 39150–39162.
210 S. M. Lehar, T. Pillow, M. Xu, L. Staben, K. K. Kajihara, R. Vandlen, L. DePalatis, H. Raab, W. L. Hazenbos, J. H. Morisaki, J. Kim, S. Park, M. Darwish, B.-C. Lee, H. Hernandez, K. M. Loyet, P. Lupardus, R. Fong, D. Yan, C. Chalouni, E. Luis, Y. Khalfin, E. Plise, J. Cheong, J. P. Lyssikatos, M. Strandh, K. Koefoed, P. S. Andersen, J. A. Flygare, M. Wah Tan, E. J. Brown and S. Mariathasan, *Nature*, 2015, **527**, 323–328.
211 W. H. Organization, *2021 Antibacterial Agents in Clinical and Preclinical development: an overview and analysis*, 2022.
212 M. Rai, K. Kon, A. Gade, A. Ingle, D. Nagaonkar, P. Paralikar and S. da Silva, *Antibiot. Resist.*, 2016, 121–143.
213 P. Karmakar and V. Gaitonde, *Medicines*, 2019, **6**, 1.
214 Y.-W. Huang, M. Cambre and H.-J. Lee, *Int. J. Mol. Sci.*, 2017, **18**, 2702.
215 E. Casals, S. Vázquez-Campos, N. G. Bastús and V. Puntes, *TrAC, Trends Anal. Chem.*, 2008, **27**, 672–683.